

Quantum capacity analysis of finite-dimensional lossy channels

Sofia Coccialetto* and Vittorio Giovannetti†
Scuola Normale Superiore, I-56126 Pisa, Italy

(Dated: January 28, 2026)

Traditionally, Quantum Information, and Quantum Communication specifically, have been focused on qubit-based architectures. Recent results, however, highlighted that higher dimensional architectures (qudit-based) may present advantages both in terms of communication and computation; a family of channels called Multi-level Amplitude Damping (MAD) channels, which are a possible qudit generalization of the well known Amplitude Damping Channels, is able to model energy decay processes that may happen during signal transmission. In this work, the Quantum Capacity of 4-dimensional MAD's is studied, relying on a technique for computing it even outside of degradable and antidegradable conditions. We also characterized the complete region of antidegradability and degradability in the parameter space for a generic d-dimensional MAD using both analytical and semi-numerical methods.

INTRODUCTION

Quantum Communication Theory (QCT) expands on the work of Shannon [1], who laid the mathematical foundations for the sharing of *classical information*, to also encompass *quantum information*. Just as we are used to think of *bits* when we think of classical messages, such as text messages, music, videos etc., QCT is traditionally focused on the sharing of *qubits* between parties across long distances; the mathematical objects that describe the transmission of quantum states are called *quantum channels*. The attention of this work is devoted to a particular class of quantum channels, i.e. *Multi-level Amplitude Damping channels*, or MAD channels, which describe an energy decay of a *qudit*, i.e. the d -dimensional equivalent of a qubit. The relevance of this kind of channels lies in their wide range of applicability: in fact, energy decays are commonplace over long distance communications, as can be exemplified by a fiber optic cable which is not completely isolated and can therefore lose a photon to the external environment. Furthermore, the focus on higher-dimensional channels, i.e. channels built upon qudit transmission, which replace the more traditional qubits, is justified by the fact that recent results highlight how these kinds of architectures may present advantages both in terms of computation [2] and communication [3].

Existing literature treated MAD channels for $d = 2$, in which case the channels are called Amplitude Damping Channels (ADC) [4] and are very well understood, and for $d = 3$ [5]. The study of 3-dimensional MAD channels [5] was carried out through an analysis of some capacity functionals, which represent the rate at which classical or quantum information can be shared when the parties involved can access possible additional resources (e.g. telephone lines, entanglement..); most importantly, the authors were able to derive the *quantum capacity* of those channels (i.e. the rate at which quantum states can be reliably transmitted through the channels), even under conditions that normally render the computation of that capacity impossible. Using the techniques first developed in the paper [5], the main objective of this work is to derive the quantum capacity for a wide range of configurations of 4-dimensional MAD channels, even when a direct computation of this quantity is normally not attainable. Furthermore, we also characterize the conditions under which MAD channels become "useless" for communicating quantum information, using semi-analytical methods that involve Semi-Definite Programming (SDP) [6]. To these ends, this work has been structured as follows:

1. derive general properties of MAD channels, with special emphasis on the case $d = 4$, see Sections I, II, III, V;
2. compute, where possible, the quantum capacities of 4-dimensional MAD channels, we explained the general process in VI and provided an example in VIA;
3. characterize the antidegradability region of MAD's, see IV

* sofia.coccialetto@sns.it

† Also at NEST, Scuola Normale Superiore and Istituto Nanoscienze-CNR, p.zza Cavalieri 7, Pisa, Italy;
vittorio.giovannetti@sns.it

Finally, in [VII A](#) we formulate a conjecture on the optimal encoding of these channels when only some of the conditions for their "uselessness" are satisfied, putting it at the test in a region of the parameter space of 3-dimensional MAD's where the quantum capacity was not known but where the conjecture allows for its computation (see [VII A 1](#)). We also note that the computations performed for the quantum capacity are also valid for the *classical private capacity*, as already shown in [\[5\]](#).

I. MAD CHANNELS IN GENERAL

Multi-level Amplitude Damping (MAD) channels are the higher-dimensional generalization of ADC channels [\[4\]](#), i.e. they are qudit-to-qudit channels describing an energy decay process, under the assumptions that the energy gaps between the levels of the qudit are all different, see [FIG. I.1](#):

$$\text{MAD} : \sigma(\mathcal{H}) \mapsto \sigma(\mathcal{H}) \quad (\text{I.1})$$

MAD's were first explored in the [\[5\]](#). Given a d -dimensional Hilbert space \mathcal{H} , spanned by the basis $\{|i\rangle\}_i$, for $i = 0, \dots, d-1$, the MAD channel has a minimal Kraus representation given by the Kraus operators:

$$\begin{aligned} K_{ij} &:= \sqrt{\gamma_{ji}} |i\rangle\langle j| \quad 0 \leq i < j \leq d-1, \\ K_{00} &:= \sum_{j=0}^{d-1} \sqrt{\gamma_{jj}} |j\rangle\langle j|. \end{aligned} \quad (\text{I.2})$$

The γ_{ji} 's in [\(I.2\)](#) describe the probabilities of decay from level $|j\rangle$ onto level $|i\rangle$, while γ_{jj} 's describe the probabilities that level $|j\rangle$ will not decay during the transformation; as such, these are real quantities satisfying:

$$\gamma_{jj} := 1 - \sum_{i=0}^{j-1} \gamma_{ji}, \quad (\text{I.3})$$

$$\begin{cases} 0 \leq \gamma_{ji} \leq 1 & \forall 0 \leq i < j \leq d-1, \\ 0 \leq \gamma_{jj} \leq 1 & \forall 0 \leq j \leq d-1, \\ \gamma_{ji} = 0 & \forall i > j. \end{cases} \quad (\text{I.4})$$

These quantities, which we name as *transition probabilities* in what follows, can be grouped into a so-called *transition matrix*, defined by:

$$\Gamma := \sum_{j=0}^{d-1} \sum_{i=0}^j \gamma_{ji} |j\rangle\langle i|, \quad (\text{I.5})$$

or, equivalently¹:

$$\Gamma := \mathbb{1}_d + \sum_{j=1}^{d-1} \sum_{i=0}^{j-1} \gamma_{ji} |j\rangle\langle i| - \sum_{j=1}^{d-1} \sum_{i=0}^{j-1} \gamma_{ji} |j\rangle\langle j|, \quad (\text{I.6})$$

where $\mathbb{1}_d$ is the d -dimensional identity matrix. There is a one-to-one relation between a specific MAD channel and its transition matrix Γ , so that it is possible to identify a MAD channel by Φ_Γ :

$$\Phi_\Gamma \sim \Gamma. \quad (\text{I.7})$$

Finally, given an input $\rho \in \sigma(\mathcal{H})$, a MAD channel Φ_Γ outputs the state:

$$\Phi_\Gamma(\rho) = K_{00}\rho K_{00}^\dagger + \sum_{j=1}^{d-1} \sum_{i=0}^{j-1} K_{ij}\rho K_{ij}^\dagger. \quad (\text{I.8})$$

Which, in terms of transition probabilities, translates to:

$$\begin{aligned} \Phi_\Gamma(\rho) = & \sum_{m=0}^{d-1} \sum_{n=0}^{d-1} \sqrt{\gamma_{mm} \gamma_{nn}} \rho_{mn} |m\rangle\langle n| \\ & + \sum_{j=1}^{d-1} \sum_{i=0}^{j-1} \gamma_{ji} \rho_{ii} |i\rangle\langle i|. \end{aligned} \quad (\text{I.9})$$

II. COMPOSITION RULES

The composition of two MAD channels is still a MAD channel:

$$\Phi_\Gamma = \Phi_{\Gamma''} \circ \Phi_{\Gamma'}. \quad (\text{II.1})$$

This is formally derived in [Appendix A.4](#), where we conclude that:

$$\Phi_\Gamma = \Phi_{\Gamma''} \circ \Phi_{\Gamma'} \Rightarrow \Gamma = \Gamma' \Gamma''. \quad (\text{II.2})$$

A. Useful decompositions

The rules [\(II.2\)](#) allow us to find various decompositions of a generic MAD channel. In what follows, we report the most useful ones for our scopes.

¹ This form can be more useful for some derivations.

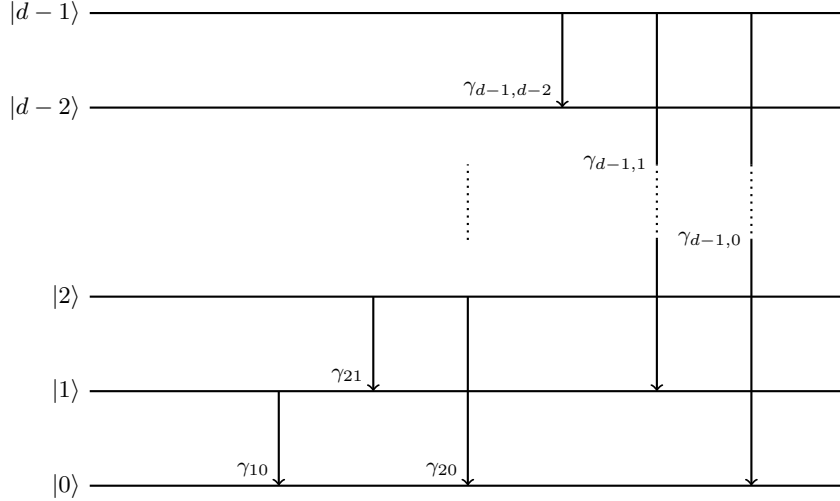


FIG. I.1: MAD channels represent decay processes, where each level of a system has a fixed probability of decaying onto a lower level. Here, a schematic depiction of a d -dimensional MAD is reported.

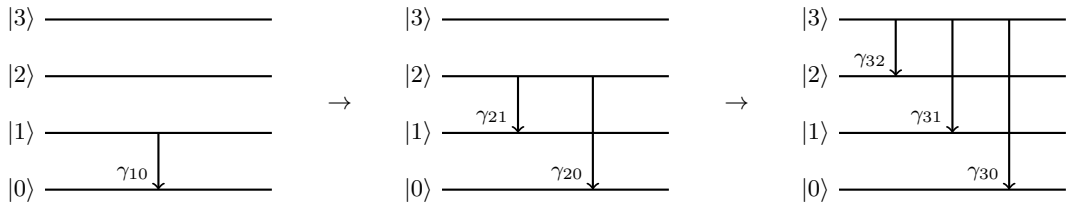


FIG. II.1: Visual representation of the decomposition of a 4-dimensional MAD channel using (II.6), to be read from left to right in "chronological" order. Thanks to (II.6), one could interpret a generic 4-dimensional MAD channel as the action of a single decay from $|1\rangle$ to $|0\rangle$, followed by a double decay from $|2\rangle$ to $|1\rangle$ and $|0\rangle$, followed by a triple decay from $|3\rangle$ to $|2\rangle$, $|1\rangle$ and $|0\rangle$.

1. Separated decays from increasing levels

in (II.3) leads to:

Define the matrices:

$$\begin{aligned} \Gamma_k &:= \mathbb{1}_d + \sum_{i=0}^{k-1} \gamma_{ki} |k\rangle\langle i| - \sum_{i=0}^{k-1} \gamma_{ki} |k\rangle\langle k|, \\ \Gamma^{(k)} &:= \mathbb{1}_d + \sum_{j=1}^{k-1} \sum_{i=0}^{j-1} \gamma_{ji} |j\rangle\langle i| - \sum_{j=1}^{k-1} \sum_{i=0}^{j-1} \gamma_{ji} |j\rangle\langle j|, \end{aligned} \quad (\text{II.3})$$

where $k < d$. Γ_k represents a special kind of MAD channel where only the level $|k\rangle$ is allowed to decay, while $\Gamma^{(k)}$ represents a MAD channel where the decays from levels $|k\rangle$ and those above it are forbidden. In this setting, the most generic d -dimensional transition matrix Γ in (I.6) is equal to $\Gamma^{(d)}$. By direct computation, setting $k = d-1$

$$\Gamma^{(d)} = \Gamma^{(d-1)} \Gamma_{d-1}, \quad (\text{II.4})$$

then, by iterating (II.4), one arrives at the decomposition:

$$\Gamma = \Gamma^{(d)} = \Gamma_1 \Gamma_2 \dots \Gamma_{d-1}, \quad (\text{II.5})$$

which, by employing (II.2), translates to:

$$\Phi_\Gamma = \Phi_{\Gamma_{d-1}} \circ \dots \circ \Phi_{\Gamma_1}. \quad (\text{II.6})$$

Intuitively speaking, (II.6) means that in a MAD channel, the lower energy levels "have precedence" when decaying, as represented in FIG. II.1.

2. MAD channels as composition of single-decay channels

Following the results in Appendix A.5, we can combine (II.5) and (A.5.8) so that we can consider a generic MAD channel as a composition of single-decay MAD channels:

$$\Gamma = \prod_{k=1}^{d-1} \left(\Xi_k^{(k-1)} \dots \Xi_k^{(0)} \right), \quad (\text{II.7})$$

where \prod_{\rightarrow} indicates that the product is meant to be expanded from left to right for increasing k 's. The (II.7) translates to:

$$\Phi_{\Gamma} = \bigodot_{k=1}^{d-1} \left(\Phi_{\Xi_k^{(0)}} \circ \dots \circ \Phi_{\Xi_k^{(k-1)}} \right), \quad (\text{II.8})$$

where \bigodot_{\leftarrow} indicates a composition of channels that is meant to be expanded from right to left for increasing k 's.

III. COMPLEMENTARY MAD CHANNEL

Complementary channels express how information is lost to the external environment during a noisy quantum evolution (refer to [7]). For complementary of MAD channels, their explicit form is found from the Kraus representations of MAD's (see e.g. [8]):

$$\begin{aligned} \tilde{\Phi}_{\Gamma}(\rho) = & \text{tr} \left(K_{00} \rho K_{00}^{\dagger} \right) |0, 0\rangle\langle 0, 0| \\ & + \left(\sum_{i < j} \text{tr} \left(K_{00} \rho K_{ij}^{\dagger} \right) |0, 0\rangle\langle i, j| + \text{h.c.} \right) \\ & + \sum_{i < j} \sum_{m < n} \text{tr} \left(K_{ij} \rho K_{mn}^{\dagger} \right) |i, j\rangle\langle m, n|, \end{aligned} \quad (\text{III.1})$$

where the sum $\sum_{i < j} = \sum_{j=1}^{d-1} \sum_{i=0}^{j-1}$. After performing the traces we end up with

$$\begin{aligned} \tilde{\Phi}_{\Gamma}(\rho) = & \sum_{j=0}^{d-1} \gamma_{jj} \rho_{jj} |0, 0\rangle\langle 0, 0| \\ & + \left(\sum_{i < j} \sqrt{\gamma_{ii} \gamma_{ji}} \rho_{ij} |0, 0\rangle\langle i, j| + \text{h.c.} \right) \\ & + \sum_{i < j} \sum_{m < n} \delta_{im} \sqrt{\gamma_{ji} \gamma_{ni}} \rho_{jn} |i, j\rangle\langle m, n|. \end{aligned} \quad (\text{III.2})$$

Note that we chose the basis of \mathcal{H}_E as:

$$\left\{ |0, 0\rangle, \{ |i, j\rangle \}_{0 \leq i < j \leq d-1} \right\}; \quad (\text{III.3})$$

we will think of the state $|0, 0\rangle$ as the lowest energy state, while the $|i, j\rangle$ are energetically ordered as follows:

$$E(|i, j\rangle) \leq E(|k, J\rangle) \quad \forall j < J, \forall k, i \quad (\text{III.4})$$

$$E(|i, j\rangle) \leq E(|k, j\rangle) \quad \forall i < k \quad (\text{III.5})$$

IV. ANTIDEGRADABILITY

The complete antidegradability (see Appendix A.2) region in the parameter space of d -dimensional MAD channels was found. Coincidentally, any MAD that does not meet these conditions has quantum capacity bigger than 0, which means that those that do meet them are the only "useless" ones in terms of communication capabilities.

$$Q(\Phi_{\Gamma}) = 0 \Leftrightarrow \Phi_{\Gamma} \text{ antidegradable} \Leftrightarrow \gamma_{j0} - \gamma_{jj} \geq 0 \quad \forall j = 1, \dots, d-1. \quad (\text{IV.1})$$

V. DEGRADABILITY

For any given d -dimensional MAD channel identified by a transition matrix Γ , we could check whether that channel is degradable (see Appendix A.2) thanks to our knowledge of the corresponding inverse map derived in Appendix

A.6, Equation (A.6.10). In fact, the degrading map is:

$$\Lambda_{\Gamma} := \tilde{\Phi}_{\Gamma} \circ \Phi_{\Gamma}^{-1}. \quad (\text{V.1})$$

By construction, this map is linear and trace-preserving, however it is not guaranteed to be completely positive. We can check that numeri-

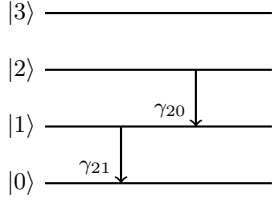


FIG. V.1: Depiction of the "problematic" ladder-like structure that renders MAD's non degradable, in the case of $d = 4$.

cally with relative ease by computing the eigenvalues of its Choi matrix (see [9], [10]). The problem of finding the complete analytical degradability conditions on the γ_{ji} 's is more complicated. The difficulty arises from the fact that the eigenvalue problem involves finding the roots of a polynomial whose degree increases with the dimensionality of the channel. We have found a working recipe that allows us to somewhat simplify the problem and through which the complete degradability region for 4-dimensional MAD channels was found.

A. Recipe for finding the degradability conditions

Here we lay out the process through which it is possible to simplify the eigenvalue problem that needs to be solved for computing the degradability region in the parameter space (i.e., the convex space generated by all the possible configurations of the γ_{ji}) for MAD channels.

1. The first step consists in a heuristic assumption: if we want the degrading map to be a quantum channel, since this map sends the output state of the laboratory system into the output state of the environment, we would expect density matrix of the latter to have rank not greater than that of the former:

$$\text{rank}(\Phi_{\Gamma}(\rho)) \geq \text{rank}(\tilde{\Phi}_{\Gamma}(\rho)) \quad \forall \rho. \quad (\text{V.2})$$

As we will see, this condition excludes some valid configurations of degradable MAD's; however, these can be recovered by extending the configurations found under the assumption (V.2).

2. The easiest way to satisfy (V.2) consists in "turning off" some of the decays: in fact, the dimensionality of the complementary

channel's output is equal to the cardinality of the minimal Kraus set of the original channel (see [11]). Therefore, we label all possible d -dimensional MAD's with at most $d - 1$ non-zero γ_{ji} 's.

3. For each of the possible classes of MAD's found in the previous step, we compute the eigenvalues of the corresponding degrading maps, resulting in the correct analytical degradability conditions for those classes.
4. Now we make use of (A.3.2); starting from the classes found earlier, we may be tempted to "turn on" other decays, purposefully violating (V.2). Can we find other degradable configurations by doing so? The answer is yes, as long as the new channel, obtained by turning on the extra decay from the degradable configurations, does not admit decompositions where one of the composing channels is not degradable. We have found that for MAD's, this reduces to excluding all the channels which present the ladder-like decay structure reported in FIG. V.1. In the case of 4-dimensional MAD's we have found the only possible 4-decay transition (that violates (V.2)) which admits degradability under certain conditions for the γ_{ji} 's.

VI. QUANTUM CAPACITY COMPUTATION FOR MAD'S: PROCEDURE

The quantum capacity Q of a quantum channel represents the rate for reliably transmitting quantum information [12]. For degradable channels, Q is relatively easy to find ([13], [14]), as they reduce to the coherent information of the channels maximized over input states:

$$\Psi \text{ is degradable} \Rightarrow Q(\Psi) = \max_{\rho \in \sigma(\mathcal{H})} I_c(\rho, \Psi). \quad (\text{VI.1})$$

Making use of the concavity of the quantum capacity over input states for degradable channels (see [15]) and the fact that, as was shown in [5], MAD channels are covariant under unitary transformations which are diagonal in the computational basis, we can prove that the maximization over input states in (VI.1) reduces to a maximization over diagonal input states in the computa-

tional basis:

$$\Phi_\Gamma \text{ is degradable} \Rightarrow Q(\Phi_\Gamma) = \max_{\substack{\rho \in \sigma(\mathcal{H}) \\ \rho \text{ diagonal}}} I_c(\rho, \Phi_\Gamma). \quad (\text{VI.2})$$

For antidegradable channels, we already know that $Q = 0$. In the case of MAD's once the degradability region is found, in that region we can compute the quantum capacity, the question is then: can we do better? In [5], the authors showcased a procedure through which they were able to compute Q for some configurations of 3-dimensional MAD channels which were neither degradable nor antidegradable. We did the same for 4-dimensional MAD channels, slightly generalizing the procedure which is summarized below:

- Find degradability conditions as seen in Section VI A.
- Compute quantum capacity in degradable conditions using (VI.2).
- Starting from a degradability condition, increase the non-zero decay probabilities so that one of the γ_{jj} 's becomes 0, then compute the quantum capacity of the resulting channel, mapping the problem to the one outlined in Section A.7 using (A.1.2), where the unitaries are level-swap unitaries.
- If the quantum capacity obtained in the last point is equal to the one at the corresponding border of the degradability condition (e.g. if we computed the capacity at $\gamma_{jj} = 0$, the corresponding border would be the one where the degradability conditions on the γ_{ji} 's are saturated), we make use of the monotonicity properties for the capacity (see Section A.8) to conclude that the region between the two borders would have the same capacity as the one computed at one of the borders.
- We iterate the last three points until possible.

In Section VI A, we provide an example to clarify the process. Note that this algorithm exploits computations of the capacity on lower-dimensional MAD's, meaning that the result found e.g. for 4-dimensional MAD's would also be useful for the capacity computations of 5, 6, ...-dimensional MAD's.

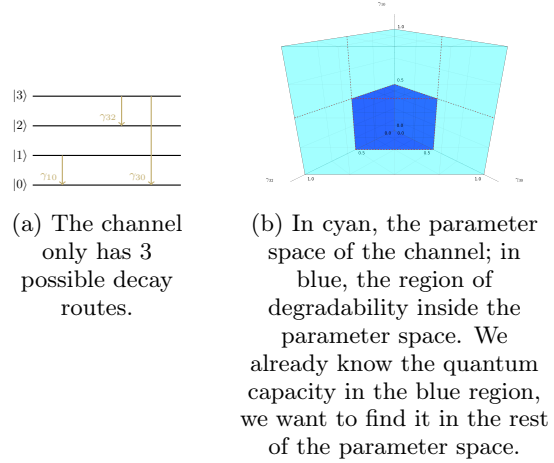


FIG. VI.1: Graphic depiction and parameter space of the MAD with transition matrix defined in (VI.3)

A. Quantum capacity computation for MAD's: example

Consider the channel depicted in FIG. VI.1 together with its parameter space and the degradability conditions. The channel is defined by the matrix:

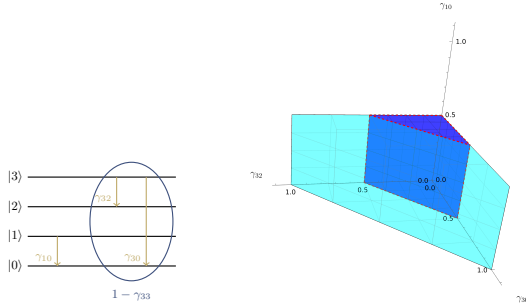
$$\begin{aligned} \Gamma = & \mathbb{1}_4 + \gamma_{10} |1\rangle\langle 0| + \gamma_{32} |3\rangle\langle 2| + \gamma_{30} |3\rangle\langle 0| \\ & - \gamma_{10} |1\rangle\langle 1| - (\gamma_{32} + \gamma_{30}) |3\rangle\langle 3|; \end{aligned} \quad (\text{VI.3})$$

its degradability conditions are:

$$\begin{aligned} \frac{1}{2} \leq \gamma_{11} \leq 1, \\ \frac{1}{2} \leq \gamma_{33} \leq 1. \end{aligned} \quad (\text{VI.4})$$

We can directly compute the quantum capacity inside the blue region in FIG. VI.1 using (VI.2) and we want to extend this computation to the cyan region.

Following the procedure highlighted above, we set $\gamma_{33} = 0$ and compute the corresponding quantum capacity (see FIG. VI.2). We can verify numerically that this is the same quantum capacity we obtain on the border of the degradability region with $\gamma_{33} = 1/2$ (as a function of γ_{10} , where $0 \leq \gamma_{10} \leq 1/2$); using the monotonicity rules outlined in Section A.8, we must conclude that in the region where $1/2 \leq \gamma_{11} \leq 1$ and $0 \leq \gamma_{33} \leq 1/2$, the quantum capacity is constant for fixed γ_{10} and can be computed on the region corresponding to $\gamma_{33} = 1/2$.



(a) We are focusing on what happens to the quantum capacity when γ_{33} changes values between 0 and $1/2$ for fixed γ_{10} .

(b) The quantum capacity on the border of the blue region $\gamma_{33} = 1/2$ is the same as that on the border of the cyan region $\gamma_{33} = 0$ for fixed γ_{10} ; therefore, the quantum capacity is constant for fixed γ_{10} in the cyan region.

FIG. VI.2: First step of extension of the computation of the quantum capacity for the MAD with transition matrix (VI.3).

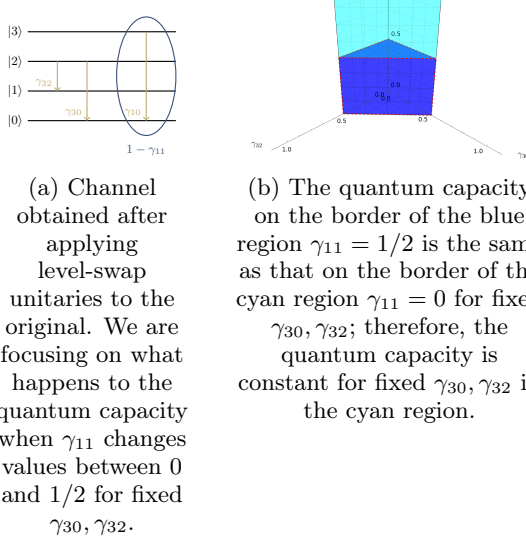


FIG. VI.3: Second step of extension of the computation of the quantum capacity for the MAD with transition matrix (VI.3).

We can repeat the same process in order to extend the computation of the quantum capacity to that region where $0 \leq \gamma_{11} \leq 1/2$ and $1/2 \leq \gamma_{33} \leq 1$; here, however, we first need to employ some level-swap unitaries to obtain a unitarily covariant channel with the same capacities as the

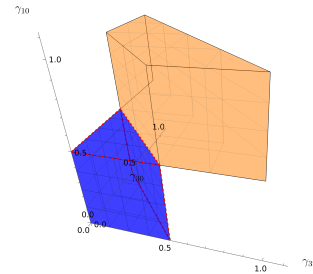


FIG. VI.4: Last step of extension of the computation of the quantum capacity for the MAD with transition matrix (VI.3). The quantum capacity, found earlier, for $\gamma_{33} = 1/2$ and $0 \leq \gamma_{11} \leq 1/2$ is 1, therefore the quantum capacity in the orange region must also be 1.

original, as depicted in FIG. VI.3. The reasoning that follows is the same as before.

Finally, we can compute the quantum capacity in the region depicted in FIG. VI.4. The quantum capacity, found earlier, for $\gamma_{33} = 1/2$ and $0 \leq \gamma_{11} \leq 1/2$ is 1; this value is also a lower bound for the quantum capacity of the channel, as we can always encode in the noiseless subspace span $\{|0\rangle, |2\rangle\}$, therefore, following the monotonicity rules, the quantum capacity in the region where $0 \leq \gamma_{11} \leq 1/2$ and $0 \leq \gamma_{33} \leq 1/2$ must be 1.

VII. CONCLUSIONS

The results of this work expanded on the previous work [5] on MAD's; we found useful general properties that aided us in the actual computation of the quantum (and, consequently, private classical) capacity of the channels (VI, VIIA). All the numerical results hinge on finding the degradability region (V) in parameter space of MAD's and comparing the value of the capacity at the external border of the degradability region against the one at the border of the parameter space, finding out that they coincide in specific instances. We were also able to compute the quantum capacity on new regions of the parameter space of 3-dimensional MAD's not yet explored (see later, VIIA 1). Finally, we formulate a conjecture on the optimal encoding of MAD's when only some of the antidegradability conditions are satisfied (see later, VIIA).

A. Conjecture

The antidegradability conditions (IV.1) provide a powerful tool for identifying "useless" channels; the level-by-level structure of the conditions tempt us to take the result one step further: what if each time a single level j degrades following $\gamma_{j0} - \gamma_{jj} \leq 0$, it means that the j level needs to be excluded in order to achieve optimal encoding? That is:

$$\exists j : \gamma_{j0} - \gamma_{jj} \leq 0 \stackrel{?}{\Rightarrow} |j\rangle \notin \text{optimal encoding.} \quad (\text{VII.1})$$

If this were true, it would mean that the quantum capacity of a d -dimensional MAD channel satisfying $\gamma_{j0} - \gamma_{jj} \leq 0$ for some j would be equal to that of a different channel which takes a $(d-1)$ -dimensional input system and outputs a d -dimensional system, and this capacity might actually be computable². This is true in those regions where we were able to actually compute the quantum capacity using the procedure illustrated in Section VI; we went back to MAD3 channel and trusted the conjecture to try and extend previous computations of the quantum capacity, resulting in what is reported in the following section.

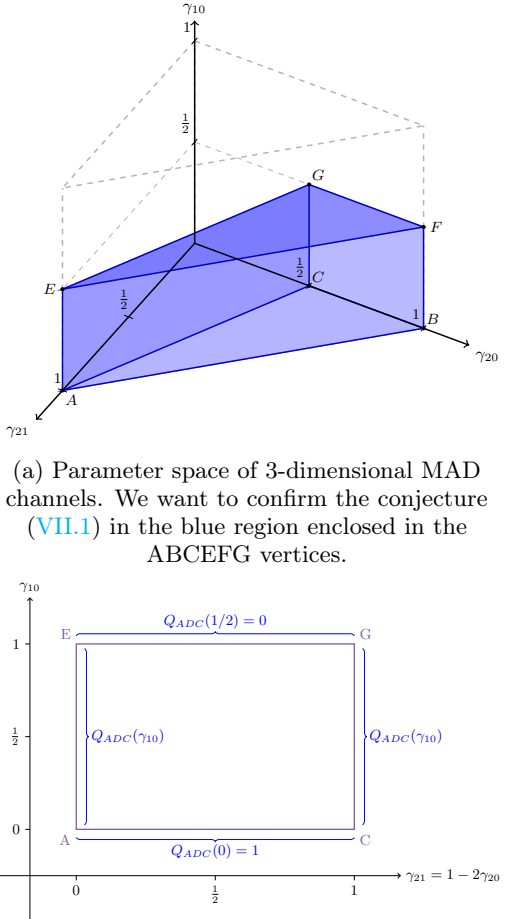
1. Back to MAD3

We tried to find the quantum capacity in the cheese-wedge region ABCDEF depicted in FIG. VII.1a. In particular, we tried to prove that the capacity on the face ABFE, which we already know to be the same as that of an amplitude damping channel with decay probability γ_{10} , is equal to that of the face ACGE:

$$Q(ACGE) = Q(ABFE) = Q_{ADC}(\gamma_{10}). \quad (\text{VII.2})$$

We already know that the quantum capacity along the edges of ACGE remains $Q_{ADC}(\gamma_{10})$ we need to prove that this also holds inside the rectangle (see FIG. VII.1b). To prove this, we fix γ_{10} , so that we can study the corresponding planar section of the parameter space in FIG. VII.1a which is depicted in FIG. VII.2a. Using the monotonicity property (A.8.3), we already know that going "up" and "down" in FIG. VII.2a

² This was the case for complete dampings in [5].



(a) Parameter space of 3-dimensional MAD channels. We want to confirm the conjecture (VII.1) in the blue region enclosed in the ABCGE vertices.

(b) Depiction of the ACGE rectangle of FIG. VII.1a. We know the capacity along its edges, we hypothesize that it will remain equal to $Q_{ADC}(\gamma_{10})$ inside the rectangle.

FIG. VII.1: Left figure is a depiction of the parameter space of 3-dimesional MAD's, right figure represents a region of that parameter space.

can only decrease the quantum capacity, so we obtain FIG. VII.2b. Following the same monotonicity rules, we also know that the capacity at fixed γ_{10} in the ACGE rectangle, represented by the purple dashed line in FIG. VII.2a has to be bigger than $Q_{ADC}(\gamma_{10})$ (see FIG. VII.3a). Now we define a new region in the parameter space, described by the relation:

$$\gamma_{21} = 1 - k\gamma_{20} \quad k \in [1, 2], \quad (\text{VII.3})$$

which corresponds to the green line in FIG. VII.2c for a given value of k ; the quantum capacity of MAD channels associated to this region

is smaller than that of MAD's in the ACGE rectangle at fixed γ_{10}, γ_{20} (see FIG. VII.3b). Now, we try to find a channel Φ_L such that:

$$\Phi_L \circ \Phi_{\Gamma_1} = \Phi_{\Gamma_2}, \quad (\text{VII.4})$$

where $\Phi_{\Gamma_1}, \Phi_{\Gamma_2}$ are MAD's corresponding to points in the purple and green regions depicted in FIG. VII.2c respectively; we can find the Choi matrix of Φ_L by using the inverse maps of MAD's (A.6.10):

$$\text{Choi}(\Phi_L) = \begin{pmatrix} 1 & 0 & 0 & 0 & 0 & 0 & \sqrt{\frac{2(k-1)(1-\omega_{21})}{k(1-\gamma_{21})}} \\ 0 & 0 & 0 & 0 & 0 & 0 & 0 \\ 0 & 0 & 0 & 0 & 0 & 0 & 0 \\ 0 & 0 & 0 & 0 & 0 & 0 & 0 \\ 1 & 0 & 0 & 0 & 0 & 0 & \sqrt{\frac{2(k-1)(1-\omega_{21})}{k(1-\gamma_{21})}} \\ 0 & 0 & 0 & 0 & 0 & 0 & 0 \\ 0 & 0 & 0 & 0 & 0 & 0 & 0 \\ 0 & 0 & 0 & 0 & 0 & 0 & 0 \\ \sqrt{\frac{2(k-1)(1-\omega_{21})}{k(1-\gamma_{21})}} & 0 & 0 & 0 & \sqrt{\frac{2(k-1)(1-\omega_{21})}{k(1-\gamma_{21})}} & 0 & \frac{2(k-1)(1-\omega_{21})}{k(1-\gamma_{21})} \end{pmatrix} \quad (\text{VII.5})$$

The non-zero eigenvalues of this matrix are:

$$\frac{2(1-\omega_{21}) - k(1-\gamma_{21})}{k(1-\gamma_{21})}, \quad \frac{2(\omega_{21} - \gamma_{21})}{1-\gamma_{21}}, \quad \frac{2k(2-\gamma_{21} - \omega_{21}) - 2(1-\omega_{21})}{k(1-\gamma_{21})}, \quad (\text{VII.6})$$

where the γ_{ji} 's are the transition probabilities of Φ_{Γ_1} while the ω_{ji} 's are those of Φ_{Γ_2} . Defining a sequence of decay probabilities:

$$\gamma_{21}^{(n)} := 1 - \frac{1}{2^n}, \quad (\text{VII.7})$$

we find that the positivity of $\text{Choi}(\Phi_L)$, under our conditions, reduces to:

$$\omega_{21}^{(n)} \leq 1 - \frac{k}{2^{n+1}}, \quad (\text{VII.8})$$

note that k can be as close to 1 as possible, albeit always being bigger than 1, so:

$$\omega_{21}^{(n)} \leq 1 - \frac{1}{2^{n+1}}. \quad (\text{VII.9})$$

Using these sequences, we can do the following: we start from $\gamma_{21}^{(0)} = 0$ and $\omega_{21}^{(0)} = 1 - k/2$, which correspond respectively to point a, a' in FIG. VII.2c; there exists a LCPT map connecting these two points through (VII.4), therefore we get that $Q_a \geq Q_{a'}$, but at the same time $Q_{a'} \geq Q_{ADC}(\gamma_{10}) = Q_a$ as this is the quantum capacity of the region in the parameter space "above" a' in FIG. VII.2c, see also FIG. VII.3c,

so $Q_a = Q_{a'}$ for all $k \in [1, 2]$, see FIG. VII.2d. Now we just need to iterate this process for $n > 0$ and we find that the quantum capacity in the entire slice of FIG. VII.2 is $Q_{ADC}(\gamma_{10})$, proving (VII.2).

APPENDIX

Appendix A.1: Unitary equivalence of channels

Consider two quantum channels Φ_1, Φ_2 which are connected by a unitary channel \mathcal{U} :

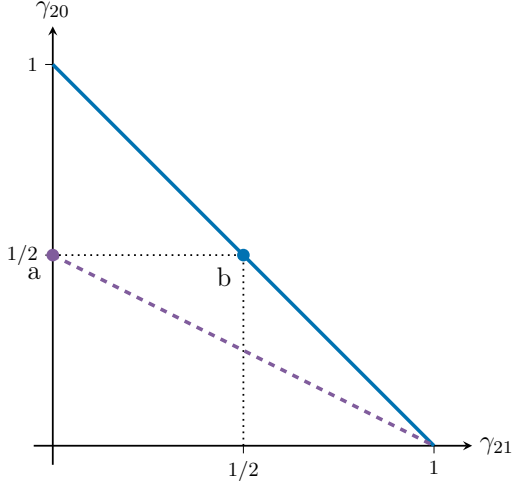
$$\mathcal{U} \circ \Phi_1 = \Phi_2 \circ \mathcal{U}; \quad (\text{A.1.1})$$

it can be shown that (see [11]), under this condition, any capacity functional \mathfrak{C} of Φ_1, Φ_2 is the same:

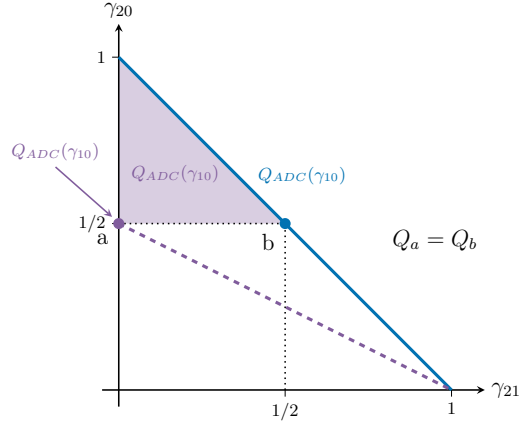
$$\begin{aligned} \exists \mathcal{U} \text{ unitary channel s.t. : } & \mathcal{U} \circ \Phi_1 = \Phi_2 \circ \mathcal{U} \\ & \Downarrow \\ & \mathfrak{C}[\Phi_1] = \mathfrak{C}[\Phi_2]. \end{aligned} \quad (\text{A.1.2})$$

In the case of MAD channels, this is particularly useful when we consider the unitary transformation to be a level swap unitary:

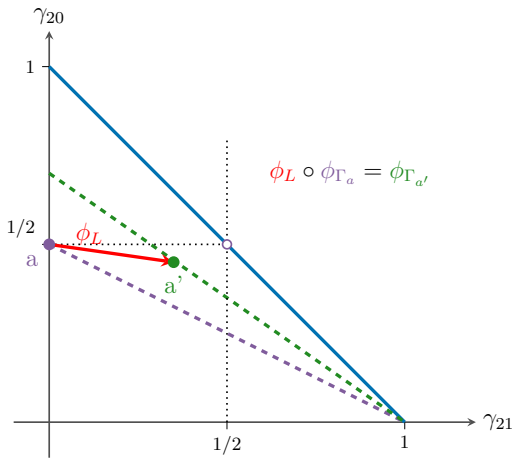
$$\begin{aligned} U_{mn} &:= \mathbb{1}_d - |m\rangle\langle m| - |n\rangle\langle n| + |m\rangle\langle n| + |n\rangle\langle m| \quad m, n \in \{0, \dots, d-1\}, \\ \mathcal{U}_{mn}(\bullet) &:= U_{mn} \bullet U_{mn}, \end{aligned} \quad (\text{A.1.3})$$



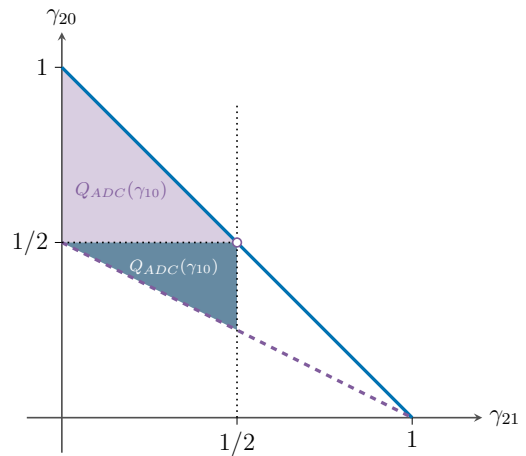
(a) The purple dashed line represent the ACGE rectangle in FIG. VII.1a, while the blue line represents the ABFE rectangle in the same figure.



(b) Using the monotonicity property (A.8.3), we can infer the quantum capacity in the upper purple triangle.



(c) The connecting channel in (VII.4) can be used to connect the two points a, a' , given by (VII.7) and (VII.8) respectively for $n = 0$ and for a value of $k \in [1, 2]$.



(d) Varying the value of k , the connecting map in FIG. VII.2c spans all the points in the lower blue triangle, allowing us to infer the value of the quantum capacity in that region (see also FIG. VII.3)

FIG. VII.2: Slice of the parameter space in FIG. VII.1a at fixed γ_{10} . These figures illustrate the first step in the algorithm used to find the quantum capacity in the entire ABCEFG cheese-wedge of FIG. VII.1a.

which swaps the levels $|m\rangle, |n\rangle$. Through this transformation, we can prove that many MAD's which are seemingly different but whose decay probabilities have the same numerical values (e.g. single decay MAD's) actually have the same ca-

pacity. Channels belonging to the same "classes" are connected through swap unitaries, so their capacity is only determined by the values of their decay rates γ_{ji} , not by the specific expression of the class.

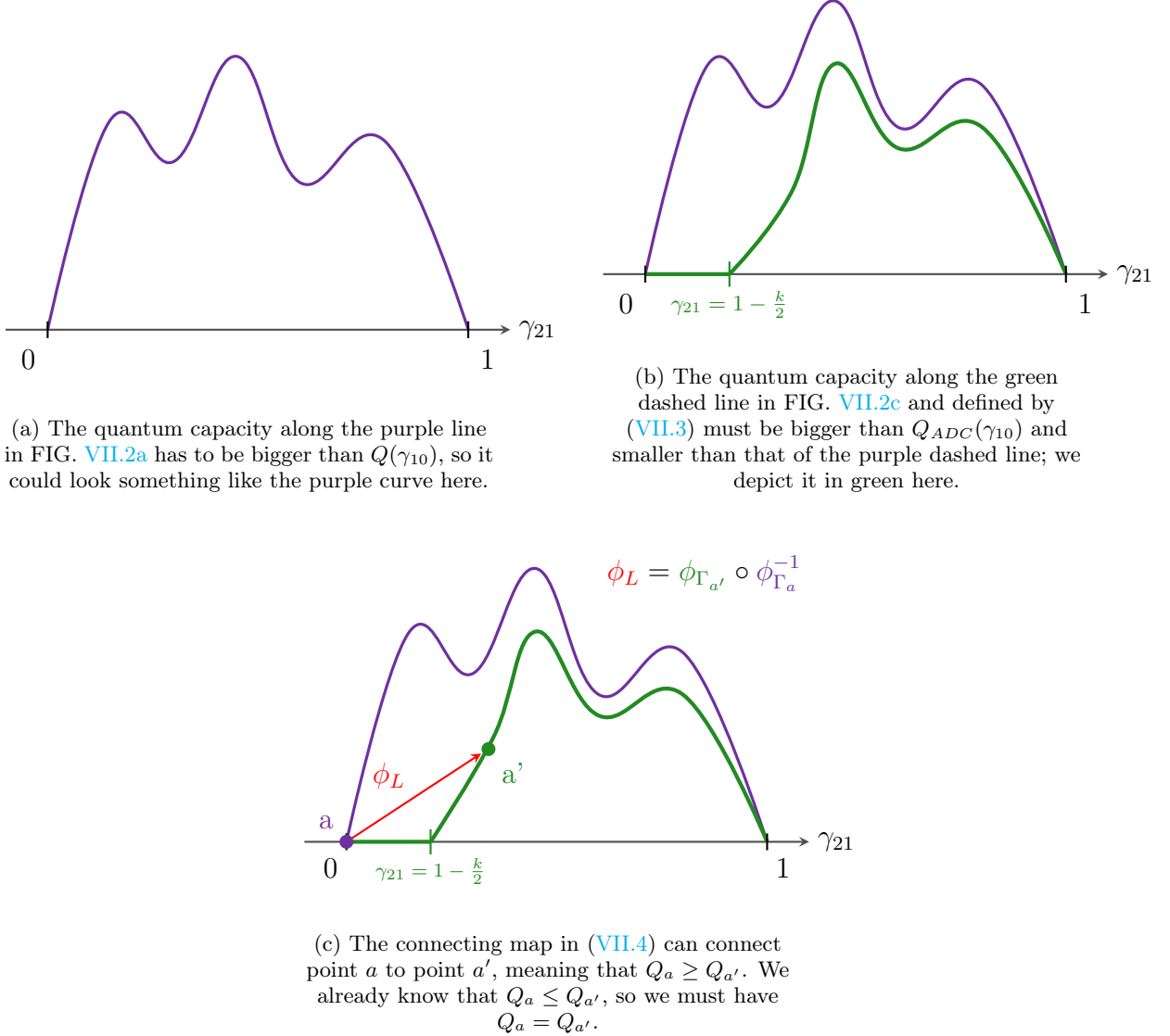


FIG. VII.3: Schematic depictions of the quantum capacity found in slices of the parameter space where the baseline corresponds to $Q_{ADC}\gamma_{10}$.

Appendix A.2: Degradability and antidegradability

A quantum channel Φ is said to be *degradable* if and only if, given its complementary channel $\tilde{\Phi}$, there exists a LCPT map Λ such that the composition $\Lambda \circ \Phi$ is equal to the complementary channel $\tilde{\Phi}$:

$$\Phi \text{ is degradable} \Leftrightarrow \exists \Lambda \text{ LCPT s.t. } \tilde{\Phi} = \Lambda \circ \Phi. \quad (\text{A.2.1})$$

Conversely Φ is said to be *antidegradable* if and only if there exists a LCPT map Λ' such that the

composition $\Lambda' \circ \tilde{\Phi}$ is equal to the channel Φ :

$$\Phi \text{ is antidegradable} \Leftrightarrow \exists \Lambda' \text{ LCPT s.t. } \Phi = \Lambda' \circ \tilde{\Phi}. \quad (\text{A.2.2})$$

FIG. A.2.1 provides a visual representation of the degradability and antidegradability conditions outlined in this section.

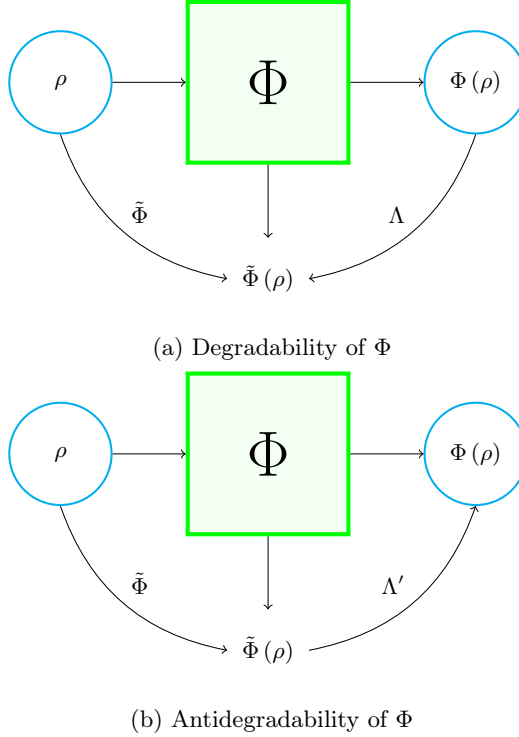


FIG. A.2.1: Visual representations for the degradability condition given in (A.2.1) and for the antidegradability condition given in (A.2.2);

Appendix A.3: Degradable channels decompositions

Given two LCPT maps Ψ_1, Ψ_2 and their composition $\Psi := \Psi_2 \circ \Psi_1$, it will be shown that:

$$\Psi = \Psi_2 \circ \Psi_1, \quad (A.3.1)$$

$$\Psi \text{ degradable} \Rightarrow \Psi_1, \Psi_2 \text{ degradable},$$

or, more eloquently:

$$\Psi = \Psi_2 \circ \Psi_1,$$

$$\exists \Lambda \text{ LCPT} : \Lambda \circ \Psi = \tilde{\Psi} \Rightarrow \begin{cases} \exists \Lambda_1 \text{ LCPT} : \Lambda_1 \circ \Psi_1 = \tilde{\Psi}_1, \\ \exists \Lambda_2 \text{ LCPT} : \Lambda_2 \circ \Psi_2 = \tilde{\Psi}_2. \end{cases} \quad (A.3.2)$$

Note that our proof hinges on the existence of a right-inverse map for Ψ_1 , as seen in the following.

a. *Tracing over single environments* Assuming that Ψ maps $\mathcal{H}_A \mapsto \mathcal{H}_B$, consider the Stinespring dilations [7] associated to the channels Ψ_1, Ψ_2 :

$$\Psi_1 \leftrightarrow V_1 : \mathcal{H}_A \mapsto \mathcal{H}_{A'} \otimes \mathcal{H}_{E_1},$$

$$\Psi_2 \leftrightarrow V_2 : \mathcal{H}_{A'} \mapsto \mathcal{H}_B \otimes \mathcal{H}_{E_2},$$

$$(A.3.3)$$

then we have that the complementary channel $\tilde{\Psi}$ of Ψ can be written as:

$$\tilde{\Psi}(\rho) = \text{tr}_{E_2} \left((V_2 \otimes \text{Id}_{E_1}) V_1 \rho V_1^\dagger (V_2^\dagger \otimes \text{Id}_{E_1}) \right). \quad (A.3.4)$$

This expression for the complementary channel is isometrically equivalent to any other valid expression (see [8]). By direct computation, it is easy to show that:

$$\begin{aligned} \text{tr}_{E_2} \tilde{\Psi}(\rho) &= \tilde{\Psi}_1(\rho), \\ \text{tr}_{E_1} \tilde{\Psi}(\rho) &= \tilde{\Psi}_2(\Psi_1(\rho)), \end{aligned} \quad (A.3.5)$$

where $\tilde{\Psi}_1, \tilde{\Psi}_2$ are respectively the complementary channels of Ψ_1, Ψ_2 .

b. *Ψ_2 is degradable* Define $\rho_1 := \Psi_1(\rho)$; using this definition, the degradability hypothesis of Ψ reads:

$$\tilde{\Psi}(\rho) = \Lambda \circ \Psi_2(\rho_1). \quad (A.3.6)$$

Applying tr_{E_1} to (A.3.6), using (A.3.5), leads to:

$$\tilde{\Psi}_2(\rho_1) = \text{tr}_{E_1} \circ \Lambda \circ \Psi_2(\rho_1). \quad (A.3.7)$$

Now, if Ψ_1 is right-invertible, i.e. \exists a map (not necessarily LCPT) Ψ_1^{-1} such that $\Psi_1 \circ \Psi_1^{-1} = \text{Id}$, by defining the LCPT $\Lambda_2 := \text{tr}_{E_1} \circ \Lambda$, we obtain:

$$\tilde{\Psi}_2 = \Lambda_2 \circ \Psi_2, \quad (A.3.8)$$

proving the degradability of Ψ_2 with a caveat that is thankfully satisfied for MAD channels, see A.6.

c. *Ψ_1 is degradable* Starting from $\tilde{\Psi} = \Lambda \circ \Psi$, we apply tr_{E_2} to both sides, using (A.3.5), obtaining:

$$\tilde{\Psi}_1 = \text{tr}_{E_2} \circ \Lambda \circ \Psi_2 \circ \Psi_1. \quad (A.3.9)$$

Then, one could define the LCPT

$$\Lambda_1 = \text{tr}_{E_2} \circ \Lambda \circ \Psi_2, \quad (A.3.10)$$

which can be substituted into (A.3.9):

$$\tilde{\Psi}_1 = \Lambda_1 \circ \Psi_1. \quad (A.3.11)$$

(A.3.11) and (A.3.8) together prove (A.3.2).

Appendix A.4: Derivation of composition rules

Consider the composition in (II.1)

$$\Phi_\Gamma = \Phi_{\Gamma''} \circ \Phi_{\Gamma'} \quad (A.4.1)$$

The matrices Γ', Γ'' have corresponding transition probabilities $\gamma'_{ji}, \gamma''_{ji}$; we want to find the function f that defines the composition rules:

$$\Gamma = f(\Gamma', \Gamma''). \quad (\text{A.4.2})$$

Expanding the right-hand side $\Phi_{\Gamma''} \circ \Phi_{\Gamma'}(\rho)$ and grouping terms in a clever way:

$$\begin{aligned} \Phi_{\Gamma''} \circ \Phi_{\Gamma'}(\rho) &= \sum_{i=0}^{l-1} \sum_{l=1}^{j-1} \sum_{j=1}^{d-1} \gamma''_{li} \gamma'_{jl} \rho_{jj} |i\rangle\langle i| + \\ &\quad \sum_{i=0}^{j-1} \sum_{j=1}^{d-1} \gamma''_{ii} \gamma'_{ji} \rho_{jj} |i\rangle\langle i| + \\ &\quad \sum_{i=0}^{j-1} \sum_{j=1}^{d-1} \gamma''_{ji} \gamma'_{jj} \rho_{jj} |i\rangle\langle i| + \\ &\quad \sum_{i=0}^{d-1} \sum_{j=1}^{d-1} \sqrt{\gamma''_{ii} \gamma'_{ii} \gamma''_{jj} \gamma'_{jj}} \rho_{ij} |i\rangle\langle j|, \end{aligned} \quad (\text{A.4.3})$$

it is possible to recognize that, if the last property in (I.4) is employed, this can be translated into:

$$\begin{aligned} \Phi_{\Gamma''} \circ \Phi_{\Gamma'}(\rho) &= \sum_{i=0}^{j-1} \sum_{j=1}^{d-1} \left(\sum_{l=0}^{d-1} \gamma''_{li} \gamma'_{jl} \right) \rho_{jj} |i\rangle\langle i| \\ &\quad + \sum_{i=0}^{d-1} \sum_{j=1}^{d-1} \sqrt{\gamma''_{ii} \gamma'_{ii} \gamma''_{jj} \gamma'_{jj}} \rho_{ij} |i\rangle\langle j|. \end{aligned} \quad (\text{A.4.4})$$

Then, the composition laws can be fixed:

$$\Phi_{\Gamma} = \Phi_{\Gamma''} \circ \Phi_{\Gamma'} \Rightarrow \gamma_{ji} = \sum_{l=0}^{d-1} \gamma'_{jl} \gamma''_{li} \quad \forall i \leq j, \quad (\text{A.4.5})$$

so that (II.1) is satisfied. Therefore, it is possible to infer that the composition of two d -dimensional MAD channels is a d -dimensional MAD channel, whose transition probabilities depend on those of the initial channels as in (A.4.5). In terms of transition matrices, (A.4.5) can easily be obtained by setting $f(\Gamma', \Gamma'') := \Gamma' \Gamma''$ in

(A.4.2), in fact:

$$\begin{aligned} \Gamma' \Gamma'' &= \sum_{j'=0}^{d-1} \sum_{i'=0}^{j'} \sum_{j''=0}^{d-1} \sum_{i''=0}^{j''} \gamma'_{j'i'} \gamma''_{j''i''} |j'\rangle\langle i'| |j''\rangle\langle i''| \\ &= \sum_{j'=0}^{d-1} \sum_{i'=0}^{d-1} \sum_{j''=0}^{d-1} \sum_{i''=0}^{d-1} \gamma'_{j'i'} \gamma''_{j''i''} |j'\rangle\langle i'| |j''\rangle\langle i''| \\ &= \sum_{j=0}^{d-1} \sum_{i=0}^{d-1} \left(\sum_{l=0}^{d-1} \gamma'_{jl} \gamma''_{li} \right) |j\rangle\langle i| \\ &\doteq \sum_{j=0}^{d-1} \sum_{i=0}^{d-1} \gamma_{ji} |j\rangle\langle i|. \end{aligned} \quad (\text{A.4.6})$$

So, the composition rules of MAD channels can be summarized by:

$$\Phi_{\Gamma} = \Phi_{\Gamma''} \circ \Phi_{\Gamma'} \Rightarrow \Gamma = \Gamma' \Gamma''. \quad (\text{A.4.7})$$

Appendix A.5: Isolate a single decay

The matrices Γ_k in (II.3) can be decomposed even further. Define the matrices:

$$\begin{aligned} \Gamma_k^{(n)} &:= \mathbb{1}_d + \gamma'_{kn} |k\rangle\langle n| - \gamma'_{kn} |k\rangle\langle k|, \\ T_k^{(n)} &:= \mathbb{1}_d + \sum_{\substack{i=0 \\ i \neq n}}^{k-1} \gamma_{ki} |k\rangle\langle i| - \sum_{\substack{i=0 \\ i \neq n}}^{k-1} \gamma_{ki} |k\rangle\langle k|, \\ T_k^{(n)} &= \Gamma_k - \gamma_{kn} |k\rangle\langle n| + \gamma_{kn} |k\rangle\langle k|, \end{aligned} \quad (\text{A.5.1})$$

where $n < k$; these matrices can be multiplied to return Γ_k if a specific value for γ'_{kn} is selected:

$$\begin{aligned} \gamma'_{kn} &:= \gamma_{kn} \left(1 - \sum_{\substack{i=0 \\ i \neq n}}^{k-1} \gamma_{ki} \right)^{-1}, \\ \Gamma_k &= T_k^{(n)} \Gamma_k^{(n)}. \end{aligned} \quad (\text{A.5.2})$$

The physical interpretation is clear: given all possible decays from the level $|k\rangle$, we can think of this process chronologically and choose the decay onto $|n\rangle$ to be performed at the end, with modified transition probabilities, as in (A.5.2); a schematic graph of this decomposition is reported in FIG. A.5.1. Note that γ'_{kn} in (A.5.2) is linear in γ_{kn} . The idea behind (A.5.2) can be expanded even further in order to create a composition of

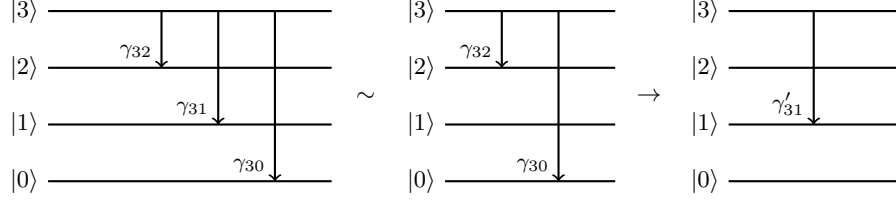


FIG. A.5.1: Example of the decomposition in (A.5.2), having fixed $k = 3, n = 1$ for 4-dimensional MAD channels, read from left to right in "chronological" order. In this case, (A.5.2) implies that the 4-dimensional MAD channel representing decays from level $|3\rangle$ onto lower levels can be decomposed by isolating a single decay, which is performed after a transition encompassing all the other decays and with a modified transition probability, defined in (A.5.2).

single transition matrices. This can be achieved by a slight redefinition of the matrices in (A.5.1):

$$\begin{aligned}\Xi_k^{(n)} &:= \mathbb{1}_d + \gamma_{kn}^{(n+1)} |k\rangle\langle n| - \gamma_{kn}^{(n+1)} |k\rangle\langle k|, \\ H_k^{(n)} &:= \mathbb{1}_d + \sum_{i=n}^{k-1} \gamma_{ki} |k\rangle\langle i| - \sum_{i=n}^{k-1} \gamma_{ki} |k\rangle\langle k|,\end{aligned}\quad (\text{A.5.3})$$

where $n < k$. The $\Xi_k^{(n)}$'s represent single decay MAD channels, from level $|k\rangle$ to $|n\rangle$, with modified amplitudes w.r.t. those of the original channel Φ_Γ , while the $H_k^{(n)}$'s represent MAD channels where only the $|k\rangle$ level can decay, with the same amplitudes as the original channel and having the transitions onto the lowest n levels forbidden. One can verify that:

$$H_k^{(0)} = \Gamma_k, \quad (\text{A.5.4})$$

which matches the descriptive definition given above. The goal here is to find the values of $\gamma_{kn}^{(n+1)}$ that allow for a useful composition of the matrices in (A.5.3). Setting the iterative equation:

$$H_k^{(n)} = H_k^{(n+1)} \Xi_k^{(n)}, \quad (\text{A.5.5})$$

leads to:

$$\begin{aligned}\gamma_{kn}^{(n+1)} &:= \frac{\gamma_{kn}}{1 - \sum_{i=n+1}^{k-1} \gamma_{ki}} \\ &= \frac{\gamma_{kn}}{\gamma_{kk} + \sum_{i=0}^n \gamma_{ki}},\end{aligned}\quad (\text{A.5.6})$$

which also implies that:

$$H_k^{(k-1)} = \Xi_k^{(k-1)}, \quad (\text{A.5.7})$$

so that:

$$\begin{aligned}\Gamma_k &= H^{(0)} = H_k^{(1)} \Xi_k^{(0)} = H_k^{(2)} \Xi_k^{(1)} \Xi_k^{(0)} \\ &= \dots = \Xi_k^{(k-1)} \dots \Xi_k^{(0)}.\end{aligned}\quad (\text{A.5.8})$$

This means that the MAD channel that allows for decays from a single level can be decomposed into a series of single transition MAD's with appropriately modified transition amplitudes.

Appendix A.6: Inverse map

Knowing the inverse map of a generic MAD channel turned out to be very useful in our computations. In this section, we report its derivation.

1. Inverse map of ADC's

The inverse map of an ADC provides a valuable guide for the derivation of the inverse MAD map. Given the ADC:

$$A_\gamma : \sigma(\mathcal{H}_2) \mapsto \sigma(\mathcal{H}_2), \quad (\text{A.6.1})$$

we denote its inverse map:

$$\begin{aligned}A_\gamma^{-1} : \sigma(\mathcal{H}_2) &\mapsto \sigma(\mathcal{H}_2), \\ A_\gamma \circ A_\gamma^{-1}(\rho) &= \rho.\end{aligned}\quad (\text{A.6.2})$$

The map A_γ^{-1} , while trace preserving and linear, is not expected to be completely positive, therefore it is likely not a quantum channel. In fact, it could be cast in a "pseudo-Kraus" representation:

$$\begin{aligned}A_\gamma^{-1}(\theta) &= \tilde{K}_0(\gamma)\theta\tilde{K}_0(\gamma)^\dagger - \tilde{K}_1(\gamma)\theta\tilde{K}_1(\gamma)^\dagger, \\ \tilde{K}_0(\gamma) &= \begin{pmatrix} 1 & 0 \\ 0 & \frac{1}{\sqrt{1-\gamma}} \end{pmatrix} \quad \tilde{K}_1(\gamma) = \begin{pmatrix} 0 & \sqrt{\frac{\gamma}{1-\gamma}} \\ 0 & 0 \end{pmatrix}.\end{aligned}\quad (\text{A.6.3})$$

Notice that, while $\tilde{K}_0(\gamma)$ and $\tilde{K}_1(\gamma)$ form a Kraus set, the "−" sign in (A.6.3) implies that A_γ^{-1} is **not** necessarily a quantum channel, as it is not written in the Kraus representation. One could also write (A.6.3) in matrix form:

$$A_\gamma^{-1}(\theta) = \begin{pmatrix} \theta_{00} - \frac{\gamma}{1-\gamma} \theta_{11} & \frac{1}{\sqrt{1-\gamma}} \theta_{01} \\ \frac{1}{\sqrt{1-\gamma}} \theta_{01}^* & \frac{1}{(1-\gamma)} \theta_{11} \end{pmatrix}. \quad (\text{A.6.4})$$

The map defined in (A.6.2) is also the left-inverse of A_γ , which can be verified by direct computation. We can see that, when $\gamma = 1$, the inverse map is not well defined, so this construction only works for $0 \leq \gamma < 1$

2. Inverse of single decay MAD channels

Consider the MAD channel $\Phi_{\Xi_k^{(n)}}$, where $\Xi_k^{(n)}$ is defined in (A.5.3) and the associated transi-

tion probability can be found in (A.5.6). This is a single decay MAD channel, which acts on the subspace spanned by $|k\rangle$ and $|n\rangle$ as an ADC with the same transition probability. Therefore, one might be tempted to define the right-inverse of $\Phi_{\Xi_k^{(n)}}$ as the embedding onto \mathcal{H}_d of the right-inverse of an ADC. Let $\Phi_{\Xi_k^{(n)}}$ be the right inverse of $\Phi_{\Xi_k^{(n)}}$. Given $\theta \in \sigma(\text{span}\{|k\rangle, |n\rangle\})$, $\Phi_{\Xi_k^{(n)}}$ needs to satisfy:

$$\Phi_{\Xi_k^{(n)}}^{-1}(\theta) = \begin{pmatrix} \theta_{nn} - \gamma_{kn}^{(n+1)} \left(1 - \gamma_{kn}^{(n+1)}\right)^{-1} \theta_{kk} & \left(1 - \gamma_{kn}^{(n+1)}\right)^{-1/2} \theta_{nk} \\ \left(1 - \gamma_{kn}^{(n+1)}\right)^{-1/2} \theta_{nk}^* & \left(1 - \gamma_{kn}^{(n+1)}\right)^{-1} \theta_{kk} \end{pmatrix}. \quad (\text{A.6.5})$$

This can be achieved by defining $\Phi_{\Xi_k^{(n)}}$ as:

$$\begin{aligned} \Phi_{\Xi_k^{(n)}}^{(-1)}(\rho) &:= \tilde{K}_0\left(\Xi_k^{(n)}\right) \rho \tilde{K}_0\left(\Xi_k^{(n)}\right)^\dagger \\ &\quad - \tilde{K}_1\left(\Xi_k^{(n)}\right) \rho \tilde{K}_1\left(\Xi_k^{(n)}\right)^\dagger, \\ \tilde{K}_0\left(\Xi_k^{(n)}\right) &:= \mathbb{1}_d - \left(1 - \left(1 - \gamma_{kn}^{(n+1)}\right)^{-1/2}\right) |k\rangle\langle k|, \\ \tilde{K}_1\left(\Xi_k^{(n)}\right) &:= \left(\frac{\gamma_{kn}^{(n+1)}}{1 - \gamma_{kn}^{(n+1)}}\right)^{1/2} |n\rangle\langle k|, \end{aligned} \quad (\text{A.6.6})$$

where $\rho \in \sigma(\mathcal{H}_d)$. It is possible to show, by direct computation, that:

$$\Phi_{\Xi_k^{(n)}} \circ \Phi_{\Xi_k^{(n)}}^{-1}(\rho) = \rho \quad \forall \rho \in \sigma(\mathcal{H}_d). \quad (\text{A.6.7})$$

Note that the map $\Phi_{\Xi_k^{(n)}}$ is linear and trace preserving and is also the left-inverse of $\Phi_{\Xi_k^{(n)}}$. Also notice that, when inverting $\Phi_{\Xi_k^{(0)}}$, since the associated decay probability is (see (A.5.6)):

$$\gamma_{k0}^{(1)} = \frac{\gamma_{k0}}{1 - \sum_{i=1}^{k-1} \gamma_{ki}} = \frac{\gamma_{k0}}{\gamma_{k0} + \gamma_{kk}}, \quad (\text{A.6.8})$$

if $\gamma_{kk} = 0$ we would get a divergence in the corresponding inverse map, given by:

$$\left(1 - \gamma_{k0}^{(1)}\right)^{-1} = 1 + \frac{\gamma_{k0}}{\gamma_{kk}}, \quad (\text{A.6.9})$$

meaning that, if $\exists k : \gamma_{kk} = 0$, the inverse map is not well defined.

3. Inverse map as composition of inverse maps of single decays

The importance of (A.6.7) lies in the fact that it can be composed to generate the right-inverse map of a general MAD channel. In fact, recall that in (II.8) it was shown that a MAD channel can be seen as a composition of single decay MAD channels. Then, by "inverting" those single decay transitions one by one, the resulting channel must be the identity channel. This line of reasoning results in the definition:

$$\Phi_\Gamma^{-1} = \bigcirc_{k=1}^{d-1} \left(\Phi_{\Xi_k^{(k-1)}}^{-1} \circ \dots \circ \Phi_{\Xi_k^{(0)}}^{-1} \right) \quad (\text{A.6.10})$$

which, by construction, satisfies:

$$\Phi_\Gamma \circ \Phi_\Gamma^{-1} = \text{Id}. \quad (\text{A.6.11})$$

Since each of the $\Phi_{\Xi_k^{(n)}}^{-1}$'s is linear and trace preserving, and a generic composition of such maps holds those same properties, then Φ_Γ^{-1} must also be linear and trace preserving. Notice, finally, that Φ_Γ^{-1} , again, by construction, is also the left inverse of Φ_Γ .

Appendix A.7: Complete damping from upper level

Consider the d -dimensional MAD channel $\Phi_{\Gamma_{\text{CD}(d-1)}}$ identified by the transition matrix:

$$\begin{aligned} \Gamma_{\text{CD}(d-1)} = \mathbb{1}_d + \sum_{j=1}^{d-1} \sum_{i=0}^{j-1} \gamma_{ji} |j\rangle\langle i| \\ - \sum_{j=1}^{d-1} \sum_{i=0}^{j-1} \gamma_{ji} |j\rangle\langle j|, \end{aligned} \quad (\text{A.7.1})$$

where $\gamma_{d-1,d-1} = 1 - \sum_{j=0}^{d-2} \gamma_{d-1,j} = 0$. The quantum capacity of this channel can be shown to be equivalent to the quantum capacity of a $d-1$ -dimensional MAD channel $\Phi_{\Gamma_{\text{MAD}(d-1)}}^{(d-1)}$, whose transition matrix is:

$$\begin{aligned} \Gamma_{\text{MAD}(d-1)} = \mathbb{1}_{d-1} + \sum_{j=1}^{d-2} \sum_{i=0}^{j-1} \gamma_{ji} |j\rangle\langle i| \\ - \sum_{j=1}^{d-2} \sum_{i=0}^{j-1} \gamma_{ji} |j\rangle\langle j|. \end{aligned} \quad (\text{A.7.2})$$

In order to reach this result, one needs to find coinciding upper and lower bounds on $Q(\Phi_{\Gamma_{\text{CD}(d-1)}})$.

1. Lower bound

The lower bound on $Q(\Phi_{\Gamma_{\text{CD}(d-1)}})$ is trivial: if one were to encode information only on the subspace spanned by $\{|0\rangle, \dots, |d-2\rangle\}$, the channel $\Phi_{\Gamma_{\text{CD}(d-1)}}$ would be equivalent to $\Phi_{\Gamma_{\text{MAD}(d-1)}}^{(d-1)}$; of course, this choice of encoding is not guaranteed to be optimal, therefore:

$$Q(\Phi_{\Gamma_{\text{CD}(d-1)}}) \geq Q(\Phi_{\Gamma_{\text{MAD}(d-1)}}^{(d-1)}). \quad (\text{A.7.3})$$

2. Upper bound

The upper bound on $Q(\Phi_{\Gamma_{\text{CD}(d-1)}})$ can be obtained using the pipeline inequalities [11]:

$$\mathfrak{C}[\Psi_2 \circ \Psi_1] \leq \min \{\mathfrak{C}[\Psi_1], \mathfrak{C}[\Psi_2]\}, \quad (\text{A.7.4})$$

where \mathfrak{C} is a capacity functional, and a result on the capacity of Direct Sum (DS) channels (see [16]):

$$Q(\Phi_{\text{CC}}^{DS}) = \max \{Q(\Phi_{\text{AA}}), Q(\Phi_{\text{BB}})\} \leq Q(\Phi_{\text{CC}}). \quad (\text{A.7.5})$$

Consider the DS channel:

$$\begin{aligned} \Phi_{\Gamma_{\text{MAD}(d-1)}}^{DS}(\theta) &:= \begin{bmatrix} \Phi_{\Gamma_{\text{MAD}(d-1)}}^{(d-1)}(p\theta^{(d-1)}) & 0 \\ 0 & 1-p \end{bmatrix}, \\ \theta &:= \begin{bmatrix} p\theta^{(d-1)} & \theta_{d-1,d-1} \\ \theta_{d-1,d-1} & 1-p \end{bmatrix}, \\ \theta &\in \sigma(\mathcal{H}_d), \theta^{(d-1)} \in \sigma(\mathcal{H}_{d-1}), \\ 0 &\leq p \leq 1, \end{aligned} \quad (\text{A.7.6})$$

and the Level Erasure channel:

$$\begin{aligned} LE_{\Gamma_{\text{CD}(d-1)}}(\rho) &:= \sum_{i \neq j}^{d-2} \rho_{ij} |i\rangle\langle j| + \sum_{i=0}^{d-2} \gamma_{d-1,i} \rho_{d-1,d-1} |i\rangle\langle i|, \\ \rho &:= \sum_{i,j=0}^{d-1} \rho_{ij} |i\rangle\langle j|, \\ \rho_{ij} &= \rho_{ji}^*, \end{aligned} \quad (\text{A.7.7})$$

where the condition found in (A.7.1) holds. The composition of these two channel is equal to $\Phi_{\Gamma_{\text{CD}(d-1)}}$:

$$\Phi_{\Gamma_{\text{CD}(d-1)}} = LE_{\Gamma_{\text{CD}(d-1)}} \circ \Phi_{\Gamma_{\text{MAD}(d-1)}}^{DS}. \quad (\text{A.7.8})$$

The quantum capacity of $\Phi_{\Gamma_{\text{MAD}(d-1)}}^{DS}$ is given in (A.7.5), which in this case translates to:

$$Q(\Phi_{\Gamma_{\text{MAD}(d-1)}}^{DS}) = Q(\Phi_{\Gamma_{\text{MAD}(d-1)}}^{(d-1)}). \quad (\text{A.7.9})$$

The pipeline inequalities (A.7.4) ensure that (A.7.9) is an upper bound for $Q(\Phi_{\Gamma_{\text{CD}(d-1)}})$:

$$Q(\Phi_{\Gamma_{\text{CD}(d-1)}}) \leq Q(\Phi_{\Gamma_{\text{MAD}(d-1)}}^{(d-1)}). \quad (\text{A.7.10})$$

Combining (A.7.3) and (A.7.10) leads to the conclusion:

$$Q(\Phi_{\Gamma_{\text{CD}(d-1)}}) = Q(\Phi_{\Gamma_{\text{MAD}(d-1)}}^{(d-1)}). \quad (\text{A.7.11})$$

Appendix A.8: Monotonicity of quantum capacity for MAD's

In [5], using the pipeline inequalities (A.7.4), the authors were able to show that the capacities of 3-dimensional MAD channels are monotonous in their parameters. In order to generalize this property of monotonicity of the capacity functionals to the d -dimensional case, one needs to consider two transition matrices, Γ, Γ' , whose elements $\gamma_{ji}, \gamma'_{ji}$ differ only for a single pair of indices (j_0, i_0) , so that:

$$\gamma'_{j_0, i_0} \geq \gamma_{j_0, i_0}. \quad (\text{A.8.1})$$

Then, on account of the pipeline inequalities (A.7.4), if we were able to find two LCPT maps Λ_L, Λ_R such that:

$$\Lambda_L \circ \Phi_\Gamma \circ \Lambda_R = \Phi_{\Gamma'}, \quad (\text{A.8.2})$$

we could conclude that the capacities MAD channels are non increasing in the parameter $\gamma'_{j_0, i_0} \geq \gamma_{j_0, i_0}$. Finding Λ_L, Λ_R is not an easy task and generally one has to resort to heuristic methods to simplify the problem. Recalling the property of closure under composition for MAD channels, one might assume that Λ_L, Λ_R are MAD's them-

selves; however, for $d > 3$, this line of reasoning only allows to derive monotonicity properties under the transition probabilities γ_{d-1, i_0} , $\forall 0 \leq i_0 < d-1$ and γ_{10} :

- **Monotonicity under γ_{d-1, i_0} :** Consider $\Lambda_R = \text{Id}_{\sigma(\mathcal{H}_d)}$ the identity channel and $\Lambda_L = \Phi_{\Gamma_{\lambda_{d-1, i_0}}}$ a single decay MAD channel from $|d-1\rangle$ to $|i_0\rangle$ with transition probability λ_{d-1, i_0} . From (II.2), the resulting channel in (A.8.2), $\Phi_{\Gamma'} = \Phi_{\Gamma_{\lambda_{d-1, i_0}}} \circ \Phi_\Gamma$ has the same transition probabilities γ'_{ji} of Φ_Γ aside from $\gamma'_{d-1, i_0} \geq \gamma_{d-1, i_0}$.
- **Monotonicity under γ_{10} :** Consider $\Lambda_L = \text{Id}_{\sigma(\mathcal{H}_d)}$ the identity channel and $\Lambda_R = \Phi_{\Gamma_{\lambda_{10}}}$ a single decay MAD channel from $|1\rangle$ to $|0\rangle$ with transition probability λ_{10} . From (II.2), the resulting channel in (A.8.2), $\Phi_{\Gamma'} = \Phi_\Gamma \circ \Phi_{\Gamma_{\lambda_{10}}}$ has the same transition probabilities γ'_{ji} of Φ_Γ aside from $\gamma'_{10} \geq \gamma_{10}$.

Combining the two cases above, we find the same result of [5], which states that the quantum capacity of 3-dimensional MAD's is monotonous non-increasing when increasing any single decay probability; in terms of (A.8.1):

$$\Phi_\Gamma, \Phi_{\Gamma'} \text{ 3-dimensional MAD's, } \gamma'_{j_0, i_0} \geq \gamma_{j_0, i_0} \Rightarrow Q(\Phi_{\Gamma'}) \leq Q(\Phi_\Gamma) \quad (\text{A.8.3})$$

1. Monotonicity properties in $d = 4$

It is unclear whether a 4-dimensional MAD channel presents monotonous capacities under the transition probabilities γ_{20}, γ_{21} . As stated above, resorting to (A.8.2) is only useful if additional assumptions are made. Assume that either one of $\Lambda_L, \Lambda_R = \text{Id}_{\sigma(\mathcal{H}_d)}$, then, utilizing the inverse map (A.6.10), from (A.8.2):

$$\Lambda_R = \text{Id}_{\sigma(\mathcal{H}_d)} \Rightarrow \Lambda_L = \Phi_{\Gamma'} \circ \Phi_\Gamma^{(-1)}, \quad (\text{A.8.4})$$

$$\Lambda_L = \text{Id}_{\sigma(\mathcal{H}_d)} \Rightarrow \Lambda_R = \Phi_\Gamma^{(-1)} \circ \Phi_{\Gamma'}. \quad (\text{A.8.5})$$

Note that, by construction, both of these maps are linear and trace preserving; verifying their complete positiveness would imply that they are quantum channels, which can be done by verifying the positive semi-definiteness of their Choi matrices, due to the Choi theorem ([9], [10]).

a. Case $\gamma'_{21} \geq \gamma_{21}$

Assume that Γ' and Γ only differ in the $|2\rangle\langle 1|$ element, so that:

$$\begin{aligned} \gamma'_{21} &:= \gamma_{21} + \varepsilon_{21} \geq \gamma_{21}, \\ 0 &\leq \varepsilon_{21} \leq \gamma_{22}, \end{aligned} \quad (\text{A.8.6})$$

where the last condition is needed in order for $\gamma_{22}' = \gamma_{22} - \varepsilon_{21} \geq 0$ to be satisfied. Computing the eigenvalues of the Choi matrices of Λ_L, Λ_R in (A.8.4) and (A.8.5), one finds that the former is only positive semi-definite if:

$$\gamma_{32} = 0, \quad (\text{A.8.7})$$

while the latter is positive semi-definite under the following condition:

$$\gamma_{20} - \gamma_{10} \geq 0, \quad (\text{A.8.8})$$

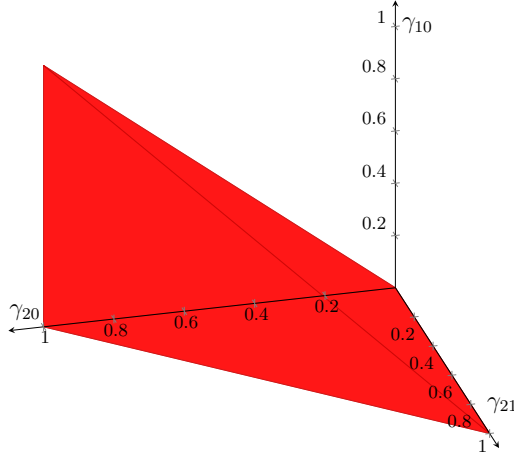


FIG. A.8.1: Monotonicity region under γ_{21} (A.8.8). Note that γ_{21}, γ_{20} are still bounded by (I.4), meaning that $0 \leq \gamma_{20} + \gamma_{21} \leq 1$.

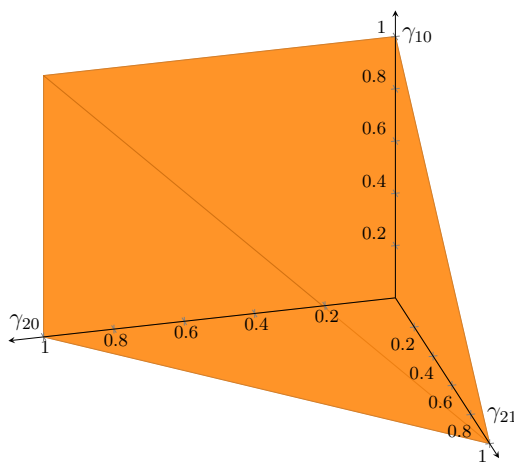


FIG. A.8.2: Monotonicity region under γ_{20} (A.8.11). Note that γ_{21}, γ_{20} are still bounded by (I.4), meaning that $0 \leq \gamma_{20} + \gamma_{21} \leq 1$.

b. Case $\gamma'_{20} \geq \gamma_{20}$

Assume that Γ' and Γ only differ in the $|2\rangle\langle 0|$ element, so that:

$$\begin{aligned} \gamma'_{20} &:= \gamma_{20} + \varepsilon_{20} \geq \gamma_{20}, \\ 0 &\leq \varepsilon_{20} \leq \gamma_{22}, \end{aligned} \quad (\text{A.8.9})$$

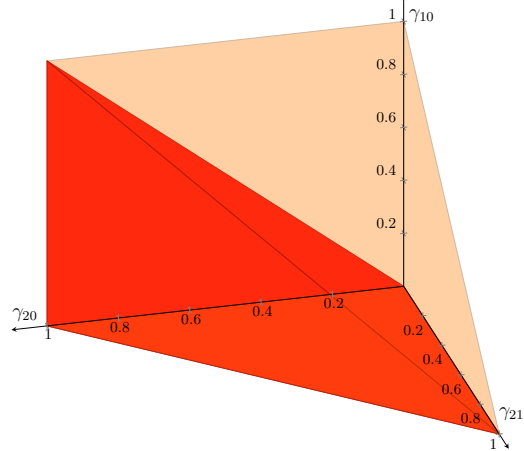


FIG. A.8.3: The monotonicity region under γ_{21} (A.8.8) is completely contained within the monotonicity region under γ_{20} (A.8.11).

where the last condition is needed in order for $\gamma_{22}' = \gamma_{22} - \varepsilon_{20} \geq 0$ to be satisfied. Computing the eigenvalues of the Choi matrices of Λ_L, Λ_R in (A.8.4) and (A.8.5), one finds that the former is only positive semi-definite if:

$$\gamma_{32} = 0, \quad (\text{A.8.10})$$

while the latter is positive semi-definite under the following condition:

$$1 - \gamma_{21} - \gamma_{10} \geq 0, \quad (\text{A.8.11})$$

which means that the capacity functionals of a 4-dimensional MAD channel are monotonous under γ_{20} if $\gamma_{32} = 0$ or $\gamma_{20} \geq \gamma_{10}$. The region described by (A.8.11) is illustrated in FIG. A.8.2. Note that the region described by (A.8.8) is completely contained within the region described by (A.8.11), as can be seen in FIG. A.8.3.

Appendix A.9: Proof of MAD antidegradability conditions

In this appendix, we provide a proof for the conditions in (IV.1)

1. Proof of sufficiency

We want to prove the following:

which means that the capacity functionals of a 4-dimensional MAD channel are monotonous under γ_{21} if $\gamma_{32} = 0$ or $\gamma_{20} \geq \gamma_{10}$. The region described by (A.8.8) is illustrated in FIG. A.8.1.

$$Q(\Phi_\Gamma) = 0 \Leftrightarrow \Phi_\Gamma \text{ antidegradable} \Leftrightarrow \gamma_{j0} - \gamma_{jj} \geq 0 \quad \forall j = 1, \dots, d-1. \quad (\text{A.9.1})$$

a. *Two-extendibility of Choi matrix*

A state ρ_{AB} in $\sigma(\mathcal{H}_A \otimes \mathcal{H}_B)$ is said to be two-extendible if there exists a state $\theta_{AB_1B_2}$ in $\sigma(\mathcal{H}_A \otimes \mathcal{H}_{B_1} \otimes \mathcal{H}_{B_2})$ that satisfies:

$$\text{tr}_{B_1} \theta_{AB_1B_2} = \rho_{AB_2} \text{ and } \text{tr}_{B_2} \theta_{AB_1B_2} = \rho_{AB_1} \quad (\text{A.9.2})$$

An important result for our scope ([17]) tells us that the Choi state ρ^Φ of a channel Φ is two-extendible if and only if Φ is antidegradable (Appendix A.2):

$$\rho^\Phi \text{ two-extendible} \Leftrightarrow \Phi \text{ antidegradable.} \quad (\text{A.9.3})$$

b. *Two-extension of Choi state for antidegradable MAD channels*

```

1  def Extendability(choi,d):
2      X = cvxpy.Variable((d**3, d**3),
3          hermitian=True) # Extension
4      constraints = [] # List of
5      constraints
6      objective = cvxpy.Minimize(np.sum(X
7          .value)) # Might set a lot of matrix
8      elements to 0
9      constraints.append(X>>0)
10     constraints.append(np_array_as_expr
11         (partial_trace(expr_as_np_array(X),
12             sys=[2], dim=3*[d]))==choi)
13     constraints.append(np_array_as_expr
14         (partial_trace(expr_as_np_array(X),
15             sys=[1], dim=3*[d]))==choi)
16
17     print("START!\n")

```

```

10
11     prob = cvxpy.Problem(objective,
12         constraints) # Initialize problem
13     prob.solve(solver=cvxpy.MOSEK,
14         verbose=False) # Call solver
15
16     if prob.status not in ["infeasible",
17         "unbounded"]:
18         print('Antidegradable.\n')
19         print(np.real(np.round(X.value,2)))
20         return 1
21     else:
22         return 0

```

Listing 1: Function to check if a Choi state choi is 2-extendable

The conditions given in (IV.1) were already suspected to be correct from the results obtained for 3, 4-dimensional MAD's. A more rigorous numerical exploration was initiated following the two-extendibility theorem (A.9.3). This was done through semi-definite programming [6] (implemented in Python), which is a very useful tool to solve minimum problems given a set of constraints. In the case at hand, we want to find out whether there exist a state that satisfies the conditions in (A.9.2) for a certain set of parameters γ_{ji} ; therefore, we are not interested in minimizing an objective function, we just want to know whether a solution is feasible. In Listing 1 the basic structure of the function used for implementing the semidefinite program is reported. Inferring from this numerical process, an analytical candidate for the two-extension of the Choi states of antidegradable MAD's was obtained. The general Choi state of a MAD channel is given by:

$$C_{AB} = \frac{1}{2} \left(\sum_{j=0}^{d-1} |j\rangle_A \langle j| \sum_{i=0}^j \gamma_{ji} |i\rangle_B \langle i| + \sum_{\substack{i,j=0 \\ i \neq j}}^{d-1} \sqrt{\gamma_{jj}\gamma_{ii}} |j\rangle_A \langle i| |j\rangle_B \langle i| \right), \quad (\text{A.9.4})$$

while it's two-extension in the antidegradable case is:

$$\tau_{AB_1B_2} = \tau_{AB_1B_2}^{\text{diag}} + \tau_{AB_1B_2}^{\text{off}}, \quad (\text{A.9.5})$$

where

$$\tau_{AB_1B_2}^{\text{diag}} := \frac{1}{d} \sum_{j=0}^{d-1} |j\rangle_A \langle j| \tau_{B_1B_2}^{(j)}, \quad (\text{A.9.6})$$

$$\begin{aligned}
\tau_{B_1 B_2}^{(j)} := & \gamma_{jj} (|0\rangle_{B_1} \langle 0| |j\rangle_{B_2} \langle j| + |j\rangle_{B_1} \langle j| |0\rangle_{B_2} \langle 0|) + \\
& \gamma_{jj} (1 - \delta_{j0}) (|0\rangle_{B_1} \langle 0| |j\rangle_{B_2} \langle 0| + |j\rangle_{B_1} \langle 0| |0\rangle_{B_2} \langle j|) + \\
& \sum_{i=1}^{j-1} \gamma_{ji} |i\rangle_{B_1} \langle i| |i\rangle_{B_2} \langle i| + \\
& |0\rangle_{B_1} \langle 0| \left(\sum_{i=0}^{j-1} p_i^{(j)} (\gamma_{j0} - \gamma_{jj}) |i\rangle_{B_2} \langle i| \right) + \\
& \sum_{i=1}^{j-1} |i\rangle_{B_1} \langle i| p_i^{(j)} (\gamma_{j0} - \gamma_{jj}) (|0\rangle_{B_2} \langle 0| - |i\rangle_{B_2} \langle i|).
\end{aligned} \tag{A.9.7}$$

$p_i^{(j)}$ is a probability distribution over the $i = 0, 1, \dots, j-1$ indices $\forall j$; the addendum in the second line vanishes when taking the partial traces. The other term is much simpler:

$$\tau_{AB_1 B_2}^{off} := \frac{1}{d} \sum_{\substack{i,j=0 \\ i \neq j}} |j\rangle_A \langle i| \sqrt{\gamma_{jj} \gamma_{ii}} \tau_{B_1 B_2}^{(ji)}, \tag{A.9.8}$$

$$\begin{aligned}
\tau_{B_1 B_2}^{(ji)} := & |0\rangle_{B_1} \langle 0| |j\rangle_{B_2} \langle i| + |j\rangle_{B_1} \langle i| |0\rangle_{B_2} \langle 0| + \\
& (1 - \delta_{j0} \delta_{i0}) (|j\rangle_{B_1} \langle 0| |0\rangle_{B_2} \langle i| + |0\rangle_{B_1} \langle i| |j\rangle_{B_2} \langle 0|).
\end{aligned} \tag{A.9.9}$$

The partial traces over the subspaces B_1, B_2 of $\tau_{AB_1 B_2}$ return the desired $C_{AB_1(B_2)}$ in (A.9.4), the only thing left to be proven is that $\tau_{AB_1 B_2}$ is actually a state, which requires checking its positivity.

Looking at (A.9.5), it is possible to recognize that it can be cast in a diagonal block matrix: in fact, many of its diagonal elements are already in an eigenspace of the matrix, namely:

$$\gamma_{ji} |j\rangle_A \langle j| |i\rangle_{B_1} \langle i| |i\rangle_{B_2} \langle i| \tag{A.9.10}$$

$$p_i^{(j)} (\gamma_{j0} - \gamma_{jj}) |j\rangle_A \langle j| |0\rangle_{B_1} \langle 0| |i\rangle_{B_2} \langle i|, \tag{A.9.11}$$

$$p_i^{(j)} (\gamma_{j0} - \gamma_{jj}) |j\rangle_A \langle j| |i\rangle_{B_1} \langle i| |0\rangle_{B_2} \langle 0|, \tag{A.9.12}$$

$$\left(\gamma_{ji} - p_i^{(j)} (\gamma_{j0} - \gamma_{jj}) \right) |j\rangle_A \langle j| |i\rangle_{B_1} \langle i| |i\rangle_{B_2} \langle i|, \tag{A.9.13}$$

$\forall j = 1, \dots, d-1$ and $\forall i = 0, \dots, j-1$. These elements, when grouped together through a unitary permutation, form the first diagonal block of $\tau_{AB_1 B_2}$, which we will call D . The other block will be called A , which in matrix form looks like:

$$A = \begin{pmatrix} 1 & \sqrt{\gamma_{11}} & \sqrt{\gamma_{11}} & \sqrt{\gamma_{22}} & \sqrt{\gamma_{22}} & \dots \\ \sqrt{\gamma_{11}} & \gamma_{11} & \gamma_{11} & \sqrt{\gamma_{11} \gamma_{22}} & \sqrt{\gamma_{11} \gamma_{22}} & \dots \\ \sqrt{\gamma_{11}} & \gamma_{11} & \gamma_{11} & \sqrt{\gamma_{11} \gamma_{22}} & \sqrt{\gamma_{11} \gamma_{22}} & \dots \\ \sqrt{\gamma_{22}} & \sqrt{\gamma_{11} \gamma_{22}} & \sqrt{\gamma_{11} \gamma_{22}} & \gamma_{22} & \gamma_{22} & \dots \\ \sqrt{\gamma_{22}} & \sqrt{\gamma_{11} \gamma_{22}} & \sqrt{\gamma_{11} \gamma_{22}} & \gamma_{22} & \gamma_{22} & \dots \\ \dots & \dots & \dots & \dots & \dots & \ddots \end{pmatrix} \tag{A.9.14}$$

$$\tau_{AB_1 B_2} \sim \begin{pmatrix} A & 0 \\ 0 & D \end{pmatrix}. \tag{A.9.15}$$

a. *Positivity of D* The matrix elements corresponding to (A.9.10) are already non-negative, while those corresponding to (A.9.11) and (A.9.12) fix the positivity conditions for D .

$$\gamma_{j0} - \gamma_{jj} \geq 0 \quad \forall j = 1, \dots, d-1. \tag{A.9.16}$$

The conditions (A.9.16) are sufficient for the positivity of (A.9.13), we just need to select the right probability distributions. Is it always possible to do so? The condition that needs to be satisfied is:

$$p_i^{(j)} \leq \frac{\gamma_{ji}}{\gamma_{j0} - \gamma_{jj}} \quad i < j; \tag{A.9.17}$$

γ_{ji} is already a probability distribution for $i = 0, 1, \dots, j$ and under our conditions (A.9.16), $\frac{\gamma_{ji}}{\gamma_{j0} - \gamma_{jj}} \geq 0$; furthermore, since $\gamma_{j0} - \gamma_{jj} \leq 1 - \gamma_{jj} \leq 1$:

$$\frac{\gamma_{ji}}{\gamma_{j0} - \gamma_{jj}} \geq \gamma_{ji} \quad \forall i < j, \tag{A.9.18}$$

therefore, the $p_i^{(j)}$'s need to be smaller than elements of another probability distribution which have been scaled up; this is obviously always possible. The only thing left to be verified is that the $p_i^{(j)}$'s can sum up to 1:

$$\sum_{i=0}^{j-1} p_i^{(j)} \leq \sum_{i=0}^{j-1} \frac{\gamma_{ji}}{\gamma_{j0} - \gamma_{jj}} = \frac{1 - \gamma_{jj}}{\gamma_{j0} - \gamma_{jj}}. \tag{A.9.19}$$

The right-hand side is bigger than 1, so the conditions (A.9.16) allow for the selection of a probability distribution $p_i^{(j)}$, meaning that the block D is positive.

b. *Positivity of A* Proving the positivity of A requires making use of Sylvester's criterion: if (and only if) all the principal minors of A are non-negative, then $A \geq 0$. Looking at A in (A.9.14), it is possible to notice that many of the principal minors will be 0; in fact, every time the submatrix obtained from A by "cutting" some rows (and corresponding columns) contains two copies of the same row, its determinant is automatically 0. This means that in order to prove the positivity of A , we only need to prove the

positivity of just one of its submatrices, specifically:

$$\tilde{A} = \begin{pmatrix} 1 & \sqrt{\gamma_{11}} & \sqrt{\gamma_{22}} & \dots \\ \sqrt{\gamma_{11}} & \gamma_{11} & \sqrt{\gamma_{11}\gamma_{22}} & \dots \\ \sqrt{\gamma_{22}} & \sqrt{\gamma_{11}\gamma_{22}} & \gamma_{22} & \dots \\ \dots & \dots & \dots & \ddots \end{pmatrix}. \quad (\text{A.9.20})$$

Computing the expectation value of \tilde{A} on a generic pure state $|\psi\rangle = \sum_i \alpha_i |i\rangle$ in the relevant d -dimensional subspace of the Hilbert space $\mathcal{H}_A \otimes \mathcal{H}_{B_1} \otimes \mathcal{H}_{B_2}$ leads to:

$$\begin{aligned} \langle \psi | \tilde{A} | \psi \rangle &= \langle \psi | \left(\left(\sum_{i=0}^{d-1} \sqrt{\gamma_{ii}} \alpha_i \right) |0\rangle + \left(\sum_{i=0}^{d-1} \sqrt{\gamma_{ii}} \alpha_i \right) \sqrt{\gamma_{11}} |1\rangle + \dots \right) \\ &= \alpha_0^* \left(\sum_{i=0}^{d-1} \sqrt{\gamma_{ii}} \alpha_i \right) + \alpha_1^* \sqrt{\gamma_{11}} \left(\sum_{i=0}^{d-1} \sqrt{\gamma_{ii}} \alpha_i \right) + \dots \\ &= \left| \sum_{i=0}^{d-1} \sqrt{\gamma_{ii}} \alpha_i \right|^2 \geq 0 \quad \forall |\psi\rangle. \end{aligned} \quad (\text{A.9.21})$$

Then $\tilde{A} \geq 0$, which means $A \geq 0$. Then, the sufficient conditions for the antidegradability of a d -dimensional MAD channel are just (A.9.16).

2. Proof of necessity

Starting from (A.9.1), in order to obtain (IV.1), one needs to prove that:

$$\exists j : \gamma_{j0} < \gamma_{jj} \Rightarrow Q(\Phi_\Gamma) > 0 \Rightarrow \Phi_\Gamma \text{ NOT antidegradable} \quad (\text{A.9.22})$$

Consider a generic MAD channel whose inputs can only be encoded on the subspace $\mathcal{H}_A := \text{span}\{|j\rangle, |0\rangle\}$. This can be thought of as a new channel $\mathcal{E} : \sigma(\mathcal{H}_A) \mapsto \sigma(\mathcal{H}_j)$, where $\mathcal{H}_j := \text{span}\{|j\rangle, |j-1\rangle, \dots, |0\rangle\}$; this channel has the same output as the original MAD channel when they are applied on inputs lying in \mathcal{H}_A . \mathcal{E} has $j+1$ Kraus operators, represented by $(j+1) \times 2$ matrices:

$$\tilde{K}_{ij} := \sqrt{\gamma_{ji}} |i\rangle\langle j| \quad 0 \leq i < j, \quad (\text{A.9.23})$$

$$\tilde{K}_{00} := |0\rangle\langle 0| + \sqrt{\gamma_{jj}} |j\rangle\langle j| \sim \begin{pmatrix} 1 & 0 \\ 0 & 0 \\ \vdots & \vdots \\ 0 & 0 \\ 0 & \sqrt{\gamma_{jj}} \end{pmatrix}. \quad (\text{A.9.24})$$

Let ρ be an element of $\sigma(\mathcal{H}_A)$:

$$\rho \sim \begin{pmatrix} 1-p & \lambda \\ \lambda^* & p \end{pmatrix}, \quad (\text{A.9.25})$$

and let $\bar{\rho} := \text{diag}(\rho)$; the output of \mathcal{E} on ρ is:

$$\begin{aligned} \mathcal{E}(\rho) &= (1-p) |0\rangle\langle 0| + \sum_{i=0}^j \gamma_{ji} p |i\rangle\langle i| + (\sqrt{\gamma_{jj}} \lambda |0\rangle\langle j| + \text{c.c.}) \\ &\sim \begin{pmatrix} (1-p) + \gamma_{j0} p & 0 & 0 & \dots & 0 & \sqrt{\gamma_{jj}} \lambda \\ 0 & \gamma_{j1} p & 0 & \dots & 0 & 0 \\ 0 & 0 & \gamma_{j2} p & & \vdots & \vdots \\ \vdots & \vdots & & \ddots & & \\ 0 & 0 & \dots & & \gamma_{j,j-1} p & 0 \\ \sqrt{\gamma_{jj}} \lambda^* & 0 & \dots & & 0 & \gamma_{jj} p \end{pmatrix}, \end{aligned} \quad (\text{A.9.26})$$

while the output of its complementary channel $\tilde{\mathcal{E}}$ on ρ is:

$$\begin{aligned} \tilde{\mathcal{E}}(\rho) &= ((1-p) + \gamma_{j0} p) |00\rangle\langle 00| + \\ &\quad \sum_{i=0}^{j-1} \gamma_{ji} p |i\rangle\langle i| + (\sqrt{\gamma_{j0}} \lambda |00\rangle\langle 0| + \text{c.c.}) \\ &\sim \begin{pmatrix} (1-p) + \gamma_{j0} p & \sqrt{\gamma_{j0}} \lambda \\ \sqrt{\gamma_{j0}} \lambda^* & \gamma_{j0} p \end{pmatrix} \begin{pmatrix} & & & & \\ & & & & \\ & & & & \\ & & & & \\ & & & & \end{pmatrix} \begin{pmatrix} & & & & \\ & & & & \\ & & & & \\ & & & & \\ & & & & \end{pmatrix} \begin{pmatrix} & & & & \\ & & & & \\ & & & & \\ & & & & \\ & & & & \end{pmatrix} \end{aligned} \quad (\text{A.9.27})$$

where $\tilde{\mathcal{E}} : \sigma(\mathcal{H}_A) \mapsto \sigma(\mathcal{H}_E)$, $\mathcal{H}_E := \text{span}\{|00\rangle, |0\rangle, \dots, |j-1\rangle\}$. As a side note here,

we can observe that, under the condition $\gamma_{j0} < \gamma_{jj}$, \mathcal{E} is degradable and the degrading channel is a MAD channel of single decay $\text{MAD}_{\omega_{j0}}$ with decay probability $\omega_{j0} := \frac{\gamma_{jj} - \gamma_{j0}}{\gamma_{jj}}$:

$$\text{MAD}_{\omega_{j0}} \circ \mathcal{E} = \tilde{\mathcal{E}}. \quad (\text{A.9.28})$$

We can try to compute a lower bound for the quantum capacity of \mathcal{E} by searching for the maximum of the coherent information on diagonal input states:

$$Q(\mathcal{E}) = \max_{\rho \in \sigma(\mathcal{H}_A)} I_C(\rho, \mathcal{E}) \geq \max_{p \in [0,1]} I_C(\bar{\rho}, \mathcal{E}). \quad (\text{A.9.29})$$

We carry out the explicit computation of $\max_{p \in [0,1]} I_C(\bar{\rho}, \mathcal{E})$:

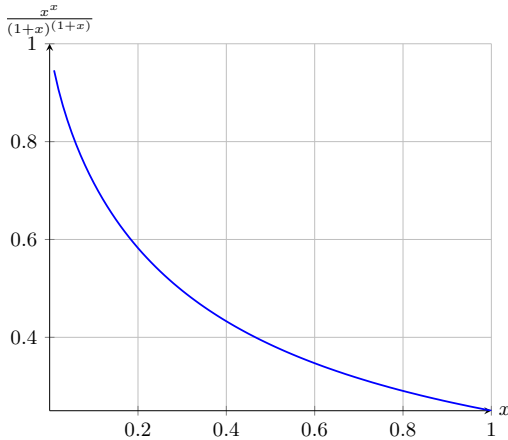


FIG. A.9.1: Plot of the function in (A.9.32)

We can now fix $p = \frac{1}{2}$, resulting in a looser lower bound for $Q(\mathcal{E})$:

$$2Q(\mathcal{E}) \geq \log_2 \left(\frac{\gamma_{j0}^{\gamma_{j0}}}{(1 + \gamma_{j0})^{(1 + \gamma_{j0})}} \right) - \log_2 \left(\frac{\gamma_{jj}^{\gamma_{jj}}}{(1 + \gamma_{jj})^{(1 + \gamma_{jj})}} \right). \quad (\text{A.9.31})$$

Given that the logarithm is a non-decreasing function and that, under our conditions, $\gamma_{j0} < \gamma_{jj}$, (A.9.31) implies that if we can prove that the function:

$$f(x) := \frac{x^x}{(1+x)^{1+x}}, \quad 0 \leq x \leq 1, \quad (\text{A.9.32})$$

is a non-increasing function, then $Q(\mathcal{E}) > 0$. We can compute the derivative of $f(x)$:

$$f'(x) = f(x) \log \left(\frac{x}{1+x} \right), \quad (\text{A.9.33})$$

since $f(x) \geq 0$ in our regime, we only require that $\log \left(\frac{x}{1+x} \right) \leq 0$, or $\frac{x}{1+x} \leq 1$, which is always true for $0 \leq x \leq 1$. Then, (A.9.22) is satisfied and so is (IV.1). A plot of $f(x)$ is reported in FIG. A.9.1.

[1] C. E. Shannon, A mathematical theory of communication, *The Bell System Technical Journal* **27**, 379 (1948).

[2] Y. Wang, Z. Hu, B. C. Sanders, and S. Kais, Qu-dits and high-dimensional quantum computing, *Frontiers in Physics* **8**, 10.3389/fphy.2020.589504 (2020).

[3] D. Cozzolino, B. Da Lio, D. Bacco, and L. K. Oxenløwe, High-dimensional quantum communication: Benefits, progress, and future challenges, *Advanced Quantum Technologies* **2**, 1900038 (2019).

- [4] V. Giovannetti and R. Fazio, Information-capacity description of spin-chain correlations, *Phys. Rev. A* **71**, 032314 (2005).
- [5] S. Chessa and V. Giovannetti, Quantum capacity analysis of multi-level amplitude damping channels, *Communications Physics* **4**, 22 (2021).
- [6] L. Vandenberghe and S. Boyd, Semidefinite programming, *SIAM Review* **38**, 49 (1996), <https://doi.org/10.1137/1038003>.
- [7] W. F. Stinespring, Positive functions on c^* -algebras, *Proceedings of the American Mathematical Society* **6**, 211 (1955).
- [8] A. S. Holevo, *Quantum Systems, Channels, Information* (De Gruyter, 2013).
- [9] M.-D. Choi, Completely positive linear maps on complex matrices, *Linear Algebra and its Applications* **10**, 285 (1975).
- [10] A. Jamiołkowski, Linear transformations which preserve trace and positive semidefiniteness of operators, *Reports on Mathematical Physics* **3**, 275 (1972).
- [11] A. S. Holevo and V. Giovannetti, Quantum channels and their entropic characteristics, *Reports on Progress in Physics* **75**, 046001 (2012).
- [12] I. Devetak, The private classical capacity and quantum capacity of a quantum channel, *IEEE Transactions on Information Theory* **51**, 44 (2005).
- [13] I. Devetak and P. W. Shor, The capacity of a quantum channel for simultaneous transmission of classical and quantum information, *Communications in Mathematical Physics* **256**, 287 (2005).
- [14] G. Smith and J. A. Smolin, Additive extensions of a quantum channel, in *2008 IEEE Information Theory Workshop* (2008) pp. 368–372.
- [15] J. Yard, P. Hayden, and I. Devetak, Capacity theorems for quantum multiple-access channels: classical-quantum and quantum-quantum capacity regions, *IEEE Transactions on Information Theory* **54**, 3091 (2008).
- [16] S. Chessa and V. Giovannetti, Partially Coherent Direct Sum Channels, *Quantum* **5**, 504 (2021).
- [17] G. O. Myhr and N. Lütkenhaus, Spectrum conditions for symmetric extendible states, *Phys. Rev. A* **79**, 062307 (2009).